RUBIES AND SAPPHIRES FROM WINZA, CENTRAL TANZANIA

Dietmar Schwarz, Vincent Pardieu, John M. Saul, Karl Schmetzer, Brendan M. Laurs, Gaston Giuliani, Leo Klemm, Anna-Kathrin Malsy, Eric Erel, Christoph Hauzenberger, Garry Du Toit, Anthony E. Fallick, and Daniel Ohnenstetter

Since late 2007, rubies and sapphires have been mined by hand methods from both eluvial and primary deposits at Winza in central Tanzania. The gem corundum is related to "dikes" of amphibolitic rocks that belong to the Paleoproterozoic Usagaran Belt. Based on crystal morphology, Winza corundum is subdivided into two types: prismatic-tabular-rhombohedral and dipyramidal. In general, medium red and dark (orangy) red top-quality rubies are rhombohedral. Pinkish red and purplish red rubies, as well as pink, purple, and blue (often strongly color zoned) sapphires are, for the most part, dipyramidal. The top-quality rubies are characterized by a distinct assemblage of long tube-, fiber-, needle-, or hair-like inclusions containing an orange-brown material (most likely limonite). The lower-quality material generally contains a larger amount of solid inclusions (mostly amphibole crystals), fissures, and growth features. Unique to corundum from this locality are bluish violet color zones oriented parallel to the prism and basal pinacoid, and occasionally also parallel to rhombohedral and dipyramidal faces. The relatively high Fe content of Winza rubies separates them from most other natural and almost all synthetic counterparts.

In early 2008, several very fine faceted rubies (e.g., figure 1) arrived in the market from a new deposit near the village of Winza in central Tanzania (Dimitri Mantheakis, pers. comm., 2008). These stones created considerable excitement, as the supply of fine unheated rubies had been scarce for years. In the ensuing gem rush, about 6,000 people had moved into the Winza area by July 2008. Although a few exceptional gems were recovered, for the most part the deposit has produced large quantities of ruby and pink-to-blue sapphire of much lower quality; very rarely, "padparadscha" sapphire is also found. Much of the material has been purchased and traded by Thai and Sri Lankan gem dealers who established buying offices in the nearby town of Mpwapwa. This report describes the mining and geology of the deposit, and provides a detailed gemological characterization of the rubies and sapphires.

Additional photos of the Winza mining area and photomicrographs of internal features are available in the *G&G* Data Depository (www.gia.edu/gemsandgemology). Also, more images and information will be available on author VP's Winza web page at www.fieldgemology.org, beginning in mid-February 2009.

HISTORY

According to Dirlam et al. (1992), ruby was first discovered in Tanzania in the early 1900s near Longido, in the northern part of the country (figure 2). At Longido and other similar Tanzanian ruby-producing localities such as Lossogonoi, the corundum is found in "anyolite," a rock composed of green zoisite and dark green to black amphibole.

In 1960, rubies and sapphires were discovered near the Kenyan border in the Umba River valley (Hänni, 1987), where desilicated pegmatites intrude serpentinite.

See end of article for About the Authors and Acknowledgments.
GEMS & GEMOLOGY, Vol. 44, No. 4, pp. 322–347.

Figure 1. Some exceptional rubies have been recovered since early 2008 from a new deposit at Winza, Tanzania. These ~5 ct and 11 ct faceted rubies are reportedly unheated, and are shown with a variety of rough samples from Winza. Courtesy of Van Cleef and Arpels, Piat, and the Gübelin Gem Lab (GGL); photo by V. Pardieu/GGL.

During the 1970s, rubies and spinels were found associated with marbles in primary or secondary deposits at two main areas in the Morogoro region of central Tanzania (Hänni and Schmetzer, 1991). The first area, located just east of the town of Morogoro near the village of Matombo, produced mainly during the 1980s. The second area is located to the south of Morogoro, near the mountain city of Mahenge. This area is quite large, and numerous ruby mining operations were known at Lukande, Mayote, Chipa, Epanko, Kitonga, and Kitwaro. The area is still being worked, but it is no longer as active as it was during the 1980s (Pardieu, 2005, 2007).

In the southern part of Tanzania, gem corundum was also found near Songea (in 1993) and Tunduru (in 1994; Milisenda et al., 1997), and these areas are still active today. However, mining declined after the discovery of the large gem placers at Ilakaka in Madagascar in 1999.

With the exception of some remarkable stones primarily from the Morogoro deposits, Tanzania was historically known to produce mostly cabochon-quality rubies or stones that required heat treatment (Dirlam et al., 1992). Therefore, the recent discovery of high-quality rubies at Winza is a welcome event for the Tanzanian gem trade.

Prior to the ruby rush, the Winza area was sparsely inhabited by maize farmers. The original discovery of ruby and sapphire there is shrouded in mystery, but some local residents report that gems were actually mined for years by a farmer who kept his activities secret. The farmer reportedly visited Dar es Salaam regularly to sell his stones. After the farmer died, his young son continued his business but was not able to keep the secret. In November 2007, Tanzanian traders learned about Winza rubies and came to the area to mine. Local reports aside, we do know that mining activities have apparently taken place in the Winza area since at least the 1950s, as evident from a Mpwapwa district map published in that decade (and seen by one of the authors [VP] in Tanzania); it showed mine symbols near the location of the present corundum deposits. Another author (JMS) recalls that in the late 1960s, large quantities of well-crystallized opaque brown-gray corundum crystals measuring up to ~10 cm were produced from near Mvomero, which is located ~100 km east of Mpwapwa, but none of the material showed potential for gem use.

By December 2007, about 600 diggers and brokers from various mining areas and gem markets in Tanzania had moved to Winza to work the deposit for ruby and sapphire. In January 2008, one of the gem brokers (Abdul Msellem) told author VP about the new deposit. At the February 2008 Tucson gem show, Tanzanian dealer Dimitri Mantheakis informed author BML that more than 1,000 miners were active in a "gem rush" to the area.

In April 2008, author VP visited Winza with gemologist Jean Baptiste Senoble, and in June author BML visited the mining area with Dr. James Shigley of GIA Research. At the time of these two visits, about 5,000 miners were working the deposit. There were numerous brokers on-site, and several buying offices had been set up in the town of Mpwapwa. By July 2008, there were more than 100

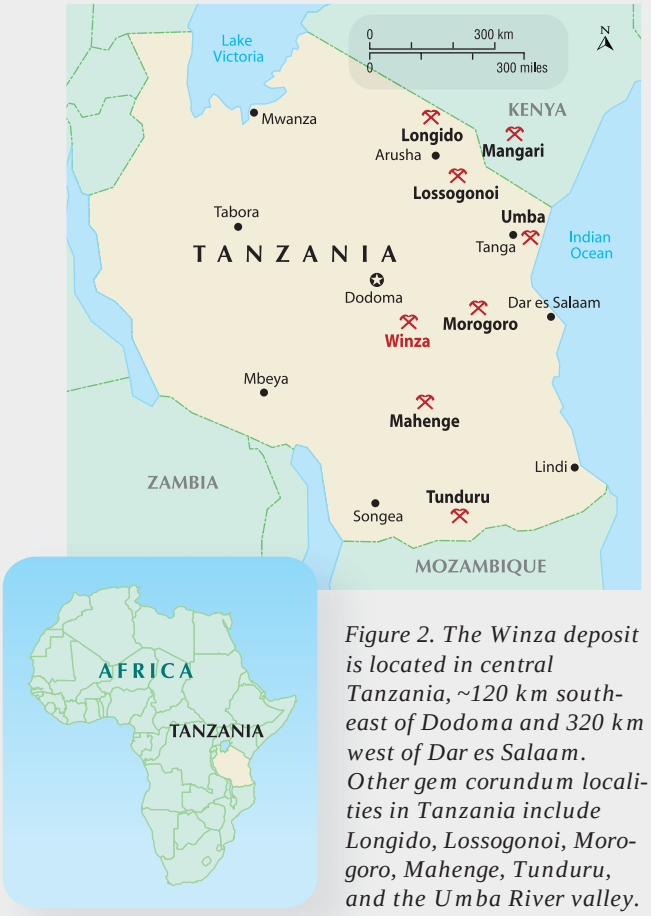

Figure 2. The Winza deposit is located in central Tanzania, ~120 km southeast of Dodoma and 320 km west of Dar es Salaam. Other gem corundum localities in Tanzania include Longido, Lossogonoi, Morogoro, Mahenge, Tunduru, and the Umba River valley.

foreign buyers (mostly Thai and Sri Lankan) in Mpwapwa and about 6,000 miners at Winza (A. Msellem, pers. comm., 2008). As of December 2008, the Tanzanian government was processing applications for 600 small-scale mining licenses (8 × 10 hectares each) in the Winza area (V. Komu, pers. comm., 2008).

LOCATION AND ACCESS

The Winza mining area is located 120 km (by air) from the capital city of Dodoma (again, see figure 2). From Dodoma, the small town of Mpwapwa is reached in about 2 hours by following a paved road for 48 km and a dirt road for 60 km. From Mpwapwa, a dirt road leads 85 km to Winza village (07°00′58′ S, 36°21′54′ E) and another 10 km to the mining area (07°05′03′ S, 36°19′11′ E). The travel time from Mpwapwa is 2.5–3 hours in a four-wheel-drive vehicle during the dry season (from approximately May to October). During the rainy season, deep mud makes the road difficult to impassable, and it may take several days to reach Winza.

The mining area is sometimes referred to as "Mtakanini" (meaning "what do you want?" in Swahili) after the name of a nearby hill. Foreigners are not allowed to visit Tanzanian gem mining areas without proper authorization from government and local authorities.

GEOLOGIC SETTING

The Winza area belongs to the Paleoproterozoic Usagaran Belt (figure 3), a rock unit composed of highly metamorphosed basement rocks, metasediments that have undergone a lower grade of metamorphism, and felsic magmatic intrusives and volcaniclastic sediments that are nearly unmetamorphosed and undeformed. Structurally, the Usagaran Belt constitutes the eastern border of the Archean Tanzania Craton (see, e.g., Fritz et al., 2005).

The eastern parts of the Usagaran Belt were reworked during the Neoproterozoic East African Orogeny and have been designated the *Western Granulites*, while further to the east, a unit of younger Mesoproterozoic rocks composed of enderbitic gneisses (metamorphosed igneous rocks of the charnockite series), schists, and marbles has been named the *Eastern Granulites* (Fritz et al., 2005). The Eastern and Western Granulites were metamorphosed simultaneously, and together they constitute the Neoproterozoic Mozambique Belt of Tanzania and Kenya.

Most of the known gem corundum occurrences in Tanzania and southeastern Kenya—including Longido, Umba, the Mangari area, Morogoro, and Mahenge—belong to the granulite-facies Eastern Granulites, which was overprinted by a metamorphic event some 620–640 million years ago (Ma) at temperatures around 750–850°C and pressures in the range of 9.5–12 kbar (Appel et al., 1998; Moeller et al., 2000; Hauzenberger et al., 2004, 2007).

At the Winza deposit, gem corundum crystals occur in mafic rocks (of unknown age), which are hosted by 1800–2000 Ma basement rocks of the Usagaran Belt (Gabert and Wendt, 1974; Sommer et al., 2005). The main rock types are migmatitic and well-foliated gneisses, indicative of upper amphibolite to granulite facies conditions. The grade of metamorphism of East African gem corundum deposits within the Eastern Granulites appears similar to that of the Usagaran basement rocks at Winza.

Mining of the primary deposits has revealed

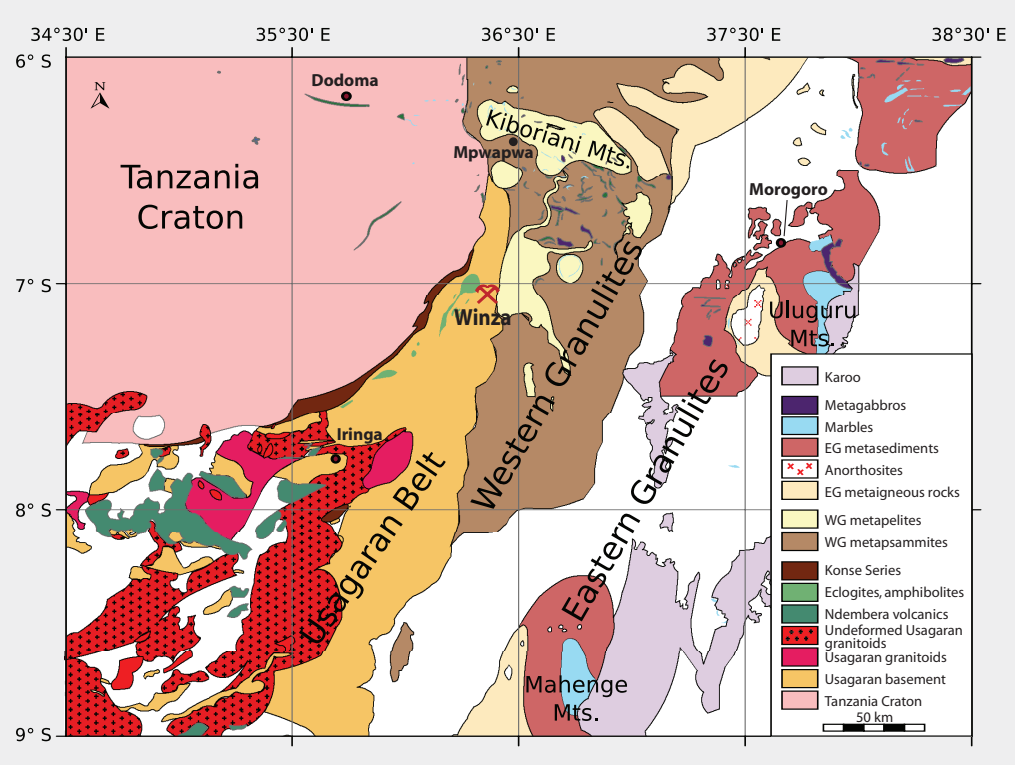

Figure 3. The Winza deposit is hosted by Usagaran basement rocks, not far from the Tanzania Craton. The basement is composed of a variety of highly metamorphosed rocks. Adapted from Fritz et al. (2005).

corundum crystals embedded within dark-colored amphibolite. Weathering of the primary deposits resulted in an overlying soil horizon (eluvial deposit) that also contains gem corundum.

MINING AND PRODUCTION

As of July 2008, mining in the Winza area was performed by several hundred small groups organized around a local miners' association. The miners constructed a settlement adjacent to the mining area, near a seasonal river (Mtindiri) that supplies water to wash the soil and for personal use. Both the eluvial and primary deposits have been worked (figure 4). The eluvial soil was excavated with picks and shovels, and taken to the river for washing. The soil was transported in bags by hand or on bicycles; a few operations also employed hand carts or pickup trucks. Although no mechanized mining was taking place, one of us (BML) saw a jigging apparatus in the mining area that was awaiting installation.

The miners use small pumps and simple screens to wash the soil (figure 5), and then pick out the gems by hand. There is little or no water in the river during the dry season, so the miners dig pits in the river bed and build dams to create small pools for their washing activities.

Work on the primary deposits was initiated in March 2008. At the time of the authors' visits, tunnels up to 30 m deep had been excavated. Material was transported to the surface using buckets that were raised by windlasses or simply by pulling ropes

Figure 4. The eluvial and primary deposits at Winza (both shown here) have been mined by hand methods, and the gem-bearing material is then carried to the Mtindiri River for washing. This is typically done by hand, but a truck was also in use at the time this photo was taken in May 2008. Photo by B. M. Laurs.

Figure 5. The gem-bearing soil is washed using water from Mtindiri River. The miners dig pits in the riverbed to make small reservoirs, and the water is pumped through a network of hoses to the washing screens. Photo by V. Pardieu/GGL.

(figure 6). Local miners informed author VP that the best-quality rubies were recovered from the eluvial deposits, although author BML was told by a similar source that at least one exceptional stone was produced from one of the tunnels in the primary deposit. During both visits, the production from the primary deposits was reported to be lower compared to the eluvial soil. As of October 2008, however, the eluvial deposits appeared to be mostly exhausted, but sapphires continued to be mined from a few tunnels in the primary deposit (A. Msellem, pers. comm., 2008).

Figure 6. Ruby and sapphire mining in Winza is now concentrating more on the primary deposit located under the gem-rich soil. Mining takes place in pits that follow near-vertical amphibolite "dikes" (one is visible here between the two workers). Photo by V. Pardieu/GGL.

Most of the Winza production is purchased at the mines by Tanzanian brokers, who typically sell the stones in Mpwapwa to foreign buyers. The buyers have constructed several offices and their advertisements are seen throughout Mpwapwa, making it reminiscent of the gem rush towns of Tunduru in southern Tanzania and Ilakaka in southern Madagascar.

Most of the Winza rough is brought to Bangkok and Colombo for distribution into the world market. Initially, heat treatment of Winza ruby was not very successful: Thai dealers reported that the stones turned orangy red without a significant improvement in color or clarity. Nevertheless, during the Gübelin Lab's off-premises testing activities at the Hong Kong Jewellery & Watch Fair in September 2008, author DS identified the first heat-treated gem-quality rubies from Winza that were submitted by customers for certification by GGL. These stones (up to ~5 ct) displayed an orange modifying hue.

Although not abundant, some very clean and highly transparent rubies—which do not need heat treatment—have been discovered at Winza (again, see figure 1). Rough material of this quality has been mistaken as synthetic by some buyers because of its strong color and transparency. Synthetics are the main problem local buyers encounter when purchasing Winza stones in Tanzania (e.g., figure 7). Also of concern is the presence of other gem materials, such as pink-red spinel, in parcels of Winza ruby.

MATERIALS AND METHODS

For this study, we characterized 289 rubies and sapphires from Winza by a variety of techniques. A description of the samples and the methods by which they were tested is given in table 1.

At GGL, we used a Topcon refractometer, with a near-sodium equivalent light source, to measure refractive indices and birefringence. Specific gravity was determined by the hydrostatic method. The fluorescence behavior to standard 365 nm long-wave and 254 nm short-wave UV radiation was observed in a darkened room. Internal features were observed with standard gemological microscopes (Bausch & Lomb and Schneider Stemi 2000 with Zeiss optics). Mineral inclusions were analyzed using a Renishaw Raman 1000 spectrometer with an Ar^+ (or green) laser at an

Figure 7. This pile of Winza ruby rough (left) formed part of a parcel offered by a Tanzanian gem broker; the small bright sample in the center turned out to be synthetic. The rough and cut samples in the right photo were seen in Dar es Salaam, and were reportedly mined from Winza. The two pieces on the left are synthetic (1.33 g rough and 1.55 ct cut), while those on the right are natural (3.89 ct cut and 0.52 g rough). Note the convincing color zoning in the rough synthetic piece. Photos by Jean Baptiste Senoble (left) and B. M. Laurs (right).

TABLE 1. Materials and methods used in this study of Winza gem corundum.

Sample group[a]	Heated?	Color	No. of samples in each group	No. of samples in each test								
				Morphology and growth structures	Standard gem properties	Internal features	Associated inclusions[b]	UV-Vis-NIR	FTIR	EDXRF	LA-ICP-MS	Isotope analysis
A1	No	Red, orange-red, purplish red, pinkish red, pink, purple, blue	1 matrix specimen	—	—	—	1 (EMPA), 1 (LA-ICP-MS)	—	—	—	—	—
A2	No		25 rough	25	—	25	3 (EMPA), 1 (XRD)	—	—	—	—	—
A3	No		70 (56+14) windowed	10	12	70	18 (Raman), 6 (LA-ICP-MS)	35	48	70	26	3
B	No	Red, orange-red, purplish red, pinkish red, padparadscha	60 faceted	20	8	60	5 (Raman)	11	11	60	20	—
C	No	Red, purplish red, orangy red	33 faceted	—	—	—	—	—	—	33	33	—
D	Yes	Orangy red	5 faceted	—	—	5	—	—	—	—	—	—
E	No/yes	Orangy red, purplish pink	3 pairs windowed	—	—	6	—	—	6	—	—	—
F	Yes	Orangy red	3 faceted	—	—	3	—	—	—	—	—	—
G1	No	Red, purplish red, purple, orangy red	25 matrix specimens	25	—	—	—	—	—	—	—	—
G2	No		50 rough	50	—	50	4 (SEM), 1 (XRD)	—	—	—	—	—
H	No	Purplish red to red	14 faceted	—	14	—	—	—	—	—	—	—

[a] *Notes:*
- *A1: Rock sample containing ruby/sapphire obtained by author JMS in Tanzania.*
- *A3: 56 samples were selected (based on color and transparency) from about 500 pieces of reportedly unheated rough obtained from miners or brokers in Mpwapwa and Arusha by one of the authors (VP) in April 2008. Fourteen samples were selected from rough material donated by various companies located in Bangkok, Colombo, and Idar-Oberstein. All samples were transparent and suitable for cutting. After two parallel windows were polished on each sample, they ranged from 0.32 to 8.71 ct.*
- *B: Most are from various companies in Thailand (~0.5–13.3 ct); includes >10 top-quality rubies submitted by GGL customers during and after the 2008 Basel Fair.*
- *C: Acquired from various companies in Thailand from April to June 2008 (~0.4–1.3 ct). All were represented as being from Winza, and their properties were consistent with the rough samples that were obtained in Tanzania by the authors.*
- *D: Examined microscopically by author DS in Bangkok in May 2008 (~0.5 ct each).*
- *E: Three untreated samples (~1.5–2.5 ct, orangy red and purplish pink) were each cut into two pieces, and then one piece from each sample was submitted for heat treatment in Bangkok in June 2008.*
- *F: Submitted to GGL gemologists for reports during the Hong Kong Jewellery & Watch Fair in September 2008 (~2–5 ct).*
- *G1 and G2: Obtained at the October 2008 Munich mineral fair.*
- *H: Submitted to the GIA Laboratory in Bangkok for reports (1.56–11.51 ct).*

[b] *Analytic technique used for identification is shown in parentheses. Abbreviations: EMPA = electron microprobe analysis, LA-ICP-MS = laser ablation–inductively coupled plasma–mass spectrometry, Raman = Raman microspectroscopy, SEM = scanning electron microscopy (with energy-dispersive spectroscopy), XRD = X-ray diffraction.*

Figure 8. The Winza rubies studied for this report include these samples (2.07–6.09 ct), which were examined at GIA's Bangkok lab in early 2008. All the stones proved to be unheated. Photo by Suchada Kittayachaiwattana.

excitation wavelength of 514 nm. Polarized ultraviolet-visible-near infrared (UV-Vis-NIR) absorption spectra were taken with a Perkin Elmer Lambda 19 spectrometer, in the range of 280–880 nm. Unpolarized mid-IR spectra (5000–1500 cm^{-1}) were collected using a Philips PU9624 Fourier-transform infrared (FTIR) spectrometer and a DRIFTS beam condenser, at a resolution of 4 cm^{-1} and with 200 scans.

Also at GGL, semiquantitative energy-dispersive X-ray fluorescence (EDXRF) chemical analysis was performed with a QuanX EC instrument (compare to Schwarz et al., 2000). It was operated using a special set of parameters optimized for the analysis of corundum with various conditions for voltage (six steps from 5–30 kV), lifetime (200–300 seconds), and filter type (no filter, cellulose, aluminum, palladium of different thickness). Laser ablation–inductively coupled plasma–mass spectrometry (LA-ICP-MS) data—approximately four spot analyses per sample—were measured with a Perkin Elmer ELAN DRC-e single collector quadrupole mass spectrometer and a CETAC LSX-213 Nd:YAG laser ablation system. The Q-switched 213 nm laser was set to a 10 Hz pulse rate with an energy of ~30 mJ per pulse of 5-nanosecond duration. All analyses were performed as single-spot (100 µm) depth profiles. In addition to the 53 faceted and 26 windowed corundum samples analyzed by this technique, the minerals in one petrographic thin section (two pale pink corundum crystals, as well as garnet and amphibole from the matrix) were analyzed by both LA-ICP-MS and electron microprobe. Electron microprobe analyses were performed at the Eugen Stumpfl Electron Microprobe Laboratory, Universities of Graz and Leoben, Austria, with a JEOL JXA 8200 instrument. Analytical conditions consisted of an accelerating voltage of 15 kV and a 10 nA sample current; matrix corrections were made following the ZAF procedure.

At GIA in Bangkok, gemological properties were measured on 14 rubies (e.g., figure 8) using standard techniques.

Crystal morphology was studied by author KS by taking angle measurements of crystals/fragments using a contact goniometer and by angle measurement in the immersion microscope.

Growth structures were observed in rough, windowed, and faceted samples by microscopic techniques with the samples immersed in methylene iodide. Five black minerals that were attached to or exposed at the surface of these samples were analyzed by scanning electron microscopy with energy-dispersive spectroscopy (SEM-EDS) and X-ray diffraction.

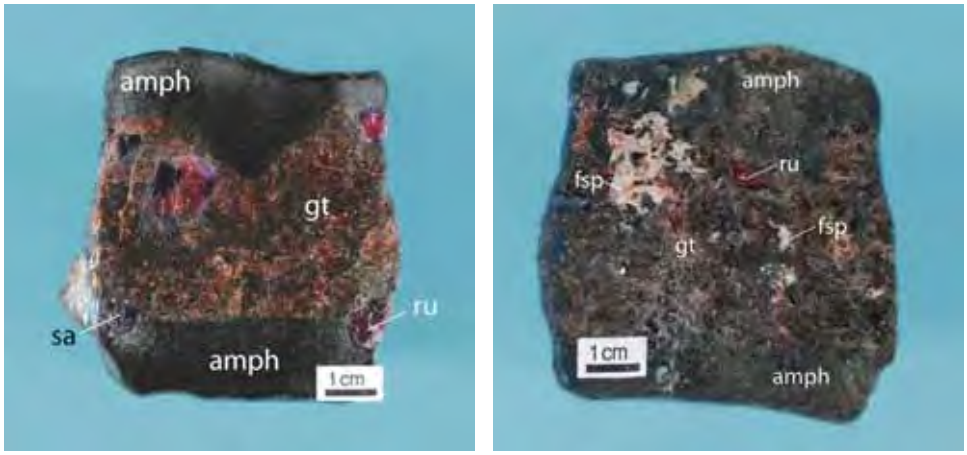

Figure 9. These slabs were cut from a Winza rock sample. The slab on the left consists of uniformly fine-grained amphibolite (amph) margins flanking orangy brown garnet (gt), ruby (ru), and sapphire (sa). The slab on the right also contains plagioclase feldspar (fsp). Photos by Patrick Lagrange.

TABLE 2. Crystal faces observed in rubies and sapphires from Winza, Tanzania.

Habit	Observed crystal form	Dominant face	Subordinate face	Miller index hkl[a]	Angle between c-axis and crystal face
Rhombohedral to prismatic	Basal pinacoid	*c*	—	(0001)	90°
	Second-order hexagonal prism	*a*	—	$(11\bar{2}0)$	0°
	Positive rhombohedron	*r*	—	$(10\bar{1}1)$	32.4°
	Negative rhombohedron	*s*	—	$(02\bar{2}1)$	17.6°
	Hexagonal dipyramid	—	*n*	$(22\bar{4}3)$	28.8°
Tabular	Basal pinacoid	*c*	—	(0001)	90°
	Negative rhombohedron	—	*s*	$(02\bar{2}1)$	17.6°
	Hexagonal dipyramid	*n*	—	$(22\bar{4}3)$	28.8°
Dipyramidal	Basal pinacoid	*c*	—	(0001)	90°
	Positive rhombohedron	—	*r*	$(10\bar{1}1)$	32.4°
	Negative rhombohedron	—	*s*	$(02\bar{2}1)$	17.6°
	Hexagonal dipyramid	*ϑ*	—	$(88\bar{1}\bar{6}3)$	7.8°
	Hexagonal dipyramid	*v*	—	$(44\bar{8}3)$	15.4°
	Hexagonal dipyramid	—	*n*	$(22\bar{4}3)$	28.8°

[a] *Based on morphological cell with a:c = 1:1.365.*

Similar nontransparent-to-semitransparent violet areas in nine rough and windowed samples from GGL were analyzed by electron microprobe (three samples) or LA-ICP-MS (six samples).

Oxygen isotope analyses of portions of three windowed GGL rubies (pink to red, deep red with blue banding, and deep red) were performed by author AEF in Scotland using a modification of the laser-fluorination technique described by Sharp (1990). Most analyses were run two or three times to check for isotopic heterogeneity and analytical artifacts. The method involved complete reaction of ~1 mg of powdered corundum, heated by a CO_2 laser, with ClF_3 as the fluorine reagent. The released oxygen was passed through an in-line Hg-diffusion pump before conversion to CO_2 on platinized graphite. The yield was measured by a capacitance manometer, and the gas-vacuum line was connected to a dedicated VG Prism 3 dual inlet isotope-ratio mass spectrometer.

Three untreated samples (~1.5–2.5 ct, orangy red and purplish pink) were each cut into two pieces, and then one piece from each sample was submitted for standard heat treatment in Bangkok in June 2008.

MINERALOGICAL AND GEMOLOGICAL PROPERTIES

Host Rock Constituents. The matrix samples consisted of corundum crystals embedded within areas of coarse-grained orangy brown garnet that are hosted by granular dark green-black amphibolite (figure 9). This assemblage locally contains areas of plagioclase, with accessory spinel, mica, kyanite, and allanite.

Electron microprobe analyses of the amphibole identified it as alumino-pargasite with a significant amount of chlorine (0.8–1.0 wt.% Cl). The chemical composition varied slightly between the core and rim and within different areas of the sample. A representative chemical formula of an amphibole core is $(Na_{0.39}K_{0.12})(Na_{0.17}Ca_{1.83})(Mg_{2.74}Fe^{2+}_{0.59}Fe^{3+}_{0.48}Al_{1.17})(Si_{5.97}Al_{2.03})O_{22}(OH_{1.72}F_{0.06}Cl_{0.22})$. The host-rock garnet was found to consist of 34% grossular, 32% pyrope, 32% almandine, and 2% spessartine, with the chemical formula $(Ca_{1.02}Mg_{0.96}Fe_{0.99}Mn_{0.1})(Al_{2.0})(SiO_4)_3$.

Corundum Crystal Morphology. All the crystals studied showed some highly reflective planar faces, but most also had less reflective, not exactly planar, and somewhat inclined and rounded faces. The latter planes were apparently contact surfaces with other corundum crystals or associated minerals. This was carefully considered when the morphology of the sometimes extremely distorted crystals was determined. Some of the crystals had distinct growth striations on their crystal faces that were oriented perpendicular to the c-axis.

The corundum crystals showed a variety of habits. Some were elongated and mostly broken, whereas others were more equidimensional, essentially complete crystals. Occasionally, elongated forms also had end faces, but complete, well-terminated crystals were extremely rare. Four habits were recognized: rhombohedral (negative and positive), prismatic (long and short), tabular, and dipyramidal. The crystal forms observed for all habits are summarized in table 2. The top-quality rubies were rhombohedral, while the lower-quality corundum was characterized by different morphology.

The rhombohedral and prismatic types were gradational into one another. No intermediate samples,

Figure 10. Most of the rhombohedral Winza ruby crystals (here, up to 13 × 18 mm) showed negative rhombohedral (pseudo-octahedral) forms, consisting of s *and* c *faces. Photo by K. Schmetzer.*

however, were observed between the rhombohedral-to-prismatic type and samples with dipyramidal habit. We saw only one tabular crystal, probably related to the positive rhombohedral type.

Surprisingly, most rhombohedral crystals consisted of the basal pinacoid *c* and the negative rhombohedron *s* as dominant forms (figure 10), rather than *c* and the positive rhombohedron *r*. The latter habit, with *c* and *r*, is commonly observed in rhombohedral corundum from Mogok, Myanmar (Bauer, 1896; Melczer, 1902), and from Morogoro, Tanzania (Hänni and Schmetzer, 1991).

*Figure 11. Several of the ruby and sapphire crystals examined (here, up to 8 × 10 mm) had positive rhombohedral faces, or both positive and negative rhombohedral forms (*r *and* s*, respectively). Depending on the size of the basal pinacoid* c*, a platy habit may result. Photo by K. Schmetzer.*

The negative rhombohedron *s* is extremely rare in corundum, though it was mentioned by Goldschmidt (1918) as a subordinate crystal form. To the best of our knowledge, *s* was not described previously as a dominant crystal form of corundum. The *r* and *s* forms can be distinguished by their different inclinations to the c-axis, which are 32.4° and 17.6°, respectively.

The angles formed by the basal pinacoid and the two rhombohedral forms were calculated as follows:

- Basal pinacoid *c* and positive rhombohedron *r*: $c\wedge r = 122.4°$, $r\wedge r = 94.0°$
- Basal pinacoid *c* and negative rhombohedron *s*: $c\wedge s = 107.6°$, $s\wedge s = 111.3°$

The two angles in corundum crystals with *c* and *s* faces are closely related to the characteristic angle of a spinel octahedron (109.5°). Therefore, this type of Winza corundum can also be described as pseudo-octahedral.

We observed only one Winza sample that showed just the *c* and *r* forms, but several intermediate samples with both *r* and *s* (figure 11). These crystals were often somewhat thick tabular (platy) in habit. Occasionally, the rhombohedral crystals also showed small hexagonal dipyramids *n*. In the one tabular sample, these faces were dominant (along with basal pinacoids) and the rhombohedral faces were subordinate.

Figure 12. These Winza corundum crystals show prismatic (far left, 11 × 7 mm) and rhombohedral-prismatic (the other four, up to 14 × 14 mm) forms, which consist of various combinations of c, a, s, r, *and* n *faces. Photo by K. Schmetzer.*

In all the prismatic Winza crystals, in addition to the basal pinacoid *c*, the hexagonal prism *a* was dominant, while *s*, *r*, and *n* faces were subordinate. According to the relative size of the *c* and *a* faces, we observed long-prismatic and short-prismatic crystals (figure 12). We also saw samples with a habit intermediate between rhombohedral and short-prismatic, some with a complicated morphology (again, see figure 12).

In contrast, samples with dipyramidal habit had simple forms. Most broken crystal fragments showed only one dipyramidal face, either ϑ or less frequently *v*. We also commonly observed *c*, occasionally in combination with small *r*, *s*, and *n* faces (figure 13). Interestingly, the dipyramidal Winza material also showed the rare negative rhombohedron *s*, but no sample with dipyramidal ϑ and *v* faces in combination with the prism *a* was observed.

The forms described above can be recognized in faceted stones by examining them in immersion and performing growth structure analysis (see below).

Figure 13. The dipyramidal Winza ruby and sapphire crystals, such as those shown here (lower right is 7 × 13 mm), are dominated by ϑ faces, which are accompanied by various combinations of c, r, s, v, *and* n *faces. Photo by K. Schmetzer.*

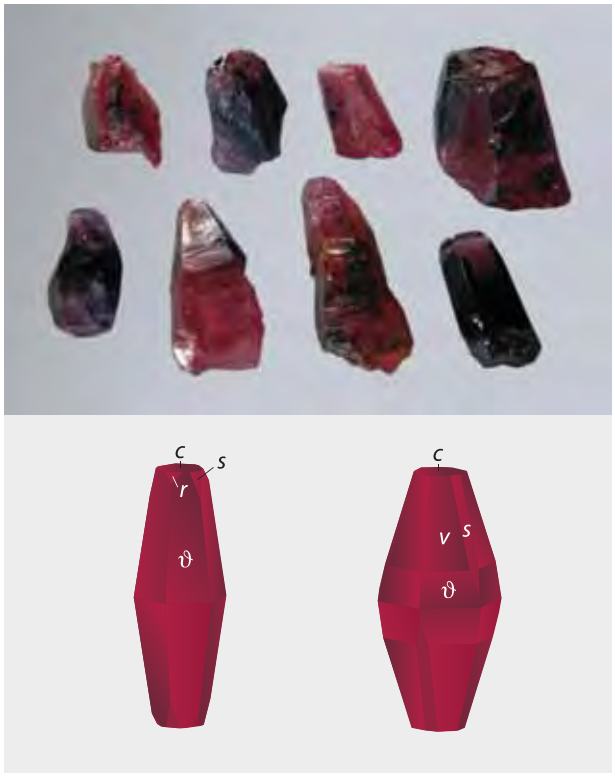

Figure 14. Note the homogeneity of color in this fine unheated 9.15 ct Winza ruby. Courtesy of Hakimi & Sons; photo by Robert Weldon.

Visual Appearance and Gemological Properties. On the basis of our faceted samples (as well as those seen in the trade), we know that Winza rubies and sapphires range from blue to red. Although some of the rubies show exceptional transparency, most Winza stones have some milkiness due to fissures and mineral inclusions. Both rubies and sapphires commonly have distinct color zoning, often with blue (or, more rarely, yellow or colorless) domains. Fine, evenly colored, saturated red or blue stones are quite rare. Top-quality vivid red rubies are generally very homogeneous in color (figure 14), but they may contain small areas of narrow blue zones. Most of the rubies are pinkish to purplish red to dark (orangy) red with moderate saturation. The sapphires are pink, purple, and blue, typically with moderate saturation (e.g., figure 15). Only a very few blue sapphires (<5 ct) of good quality from Winza have been reported in the Thai market. Orange-pink padparadscha Winza sapphires are even rarer. Our heat-treated specimens were orangy red to orange-red. Some stones cut from Winza material (unheated and heated) show more than one color (e.g., figure 16).

The physical properties of some unheated samples are reported in table 3; there were no variations in their characteristics according to color.

Growth Features and Color Zoning. Growth planes were observed parallel to the dominant crystal faces in all morphological types. However, in most of the faceted samples examined, growth zoning was only seen parallel to the basal pinacoid *c*; rarely, it was parallel to several dominant faces (figure 17). Also uncommon was color zoning in completely red or pink samples (i.e., consisting of red or pink layers of various intensity; figure 18).

Figure 15. The faceted cushion cut (1.50 ct, courtesy of Mark Kaufman) and dipyramidal crystal (2.3 cm tall, courtesy of Werner Radl) provide attractive examples of sapphires from Winza; photo by Robert Weldon. The inset photos show color variations within a dipyramidal Winza sapphire crystal (1.3 cm tall, photo by Werner Radl) and in various faceted rubies and sapphires (0.61–1.69 ct; photo by K. Schmetzer).

The samples typically showed characteristic growth and color zoning consisting of bluish violet lamellae in otherwise uniformly colored red, pink, orange-pink, or pinkish violet corundum. These lamellae were observed occasionally in rhombohedral and prismatic samples, and frequently in dipyramidal rubies and sapphires. Distinct lamellar zoning was easily seen—even with the naked eye—only in prismatic samples. Viewing perpendicular or oblique to the planes of these lamellae caused them to become transparent bluish violet. In contrast, when viewed parallel to the lamellar direction, the lamellae typically appeared black and nontransparent. Only in immersion, with proper orientation of the samples, did the fine lamellar nature of the color zoning become sharp in all samples (e.g., figure 19). Thus, such viewing conditions were necessary to resolve nonstructured color patches into fine lamellar patterns. In samples with bluish violet lamellae oriented parallel to several forms, the appearance of the color zones was rather complex (e.g., figure 20).

In prismatic crystals, the sharp bluish violet layers were typically oriented parallel to the dominant prism *a* (again, see figure 19). The pattern in rhombohedral and dipyramidal samples, however, was more complex. Viewed parallel to the c-axis, the dark bluish violet zone appeared confined to the outer rim of the crys-

Figure 16. Some Winza sapphires have been cut to show more than one color. These heat-treated samples weigh 0.88 and 1.03 ct. Courtesy of Michael Nemeth; photo by Robert Weldon.

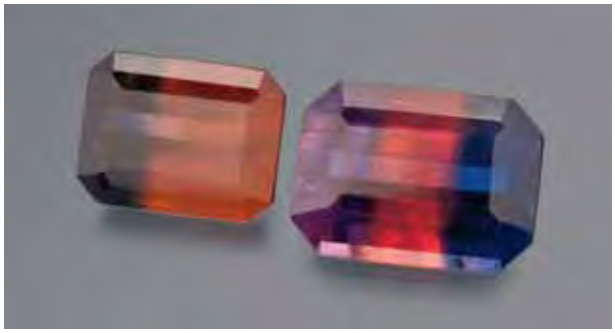

TABLE 3. Physical properties of Winza corundum.

Property	Unheated ruby and sapphire
Color	Red, purplish red, pinkish red, orangy red Blue, pink, padparadscha
Dichroism (ruby)	
e-ray (or E ∥ c)	Orange to orangy red
o-ray (or E ⊥ c)	Purple-red to violet-red
RI	
n_o	1.767–1.771
n_e	1.758–1.762
Birefringence	0.008–0.010
SG	4.00–4.03 (average 4.02)
UV fluorescence	
Long-wave	Mostly weak to moderate; top-quality rubies strong to moderately strong
Short-wave	Very weak to weak; rarely, inert
Spectroscope	Typical chromium spectrum; in part, also Fe^{3+}-related features
Internal features	• Long (typically curved) tube-, fiber-, needle- or hair-like inclusions of orange-brown color; common in top-quality red material, but not seen in pink, purple, or blue stones • Inclusion association: amphibole + garnet + apatite (rare) • Partially healed fissures composed of cavities containing mostly a polyphase filling of solid material • Fissures containing a grayish white to pale yellow substance resembling flux residues in synthetic rubies • Color zoning with thin bluish violet lamellae in both ruby and sapphire; various types of bluish violet layers parallel to the prism and/or the basal pinacoid • Rhombohedral twin planes, possibly with intersection tubules in one or more directions) • Minute (exsolved?) particles

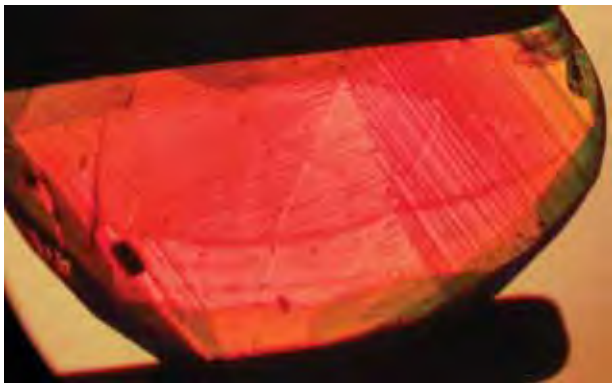

Figure 17. Multiple directions of growth zoning are rare in faceted Winza corundum. This stone has growth lines parallel to a *(center of the sample),* c *(right portion), and a small zone parallel to* n *(left side). Photomicrograph by K. Schmetzer; immersion, magnified 40× and viewed ⊥ to the c-axis.*

tals (figure 21, left; a similar crystal was documented by Choudhary, 2008). Viewed perpendicular to the c-axis, however, the bluish violet zones were seen to be localized within specific areas, separated by "normal" zones of ruby or sapphire (figure 21, center). On rotation, the intercalated "normal" layers may cause the bluish violet zones to appear as parallel layers oriented perpendicular to the c-axis (figure 21, right).

Nature of Dark-Colored Rims/Zones. Distinct bluish violet, almost black color zoning is common in Winza rubies and pink sapphires (Hänni and Krzemnicki, 2008; Krzemnicki and Hänni, 2008; Peretti 2008; Senoble, 2008). Abduriyim and Kitawaki (2008) mentioned that this color zoning is similar to the

Figure 19. Viewed parallel to the c-axis, this 13.8 × 8.3 mm slab of prismatic Winza sapphire shows distinct bluish violet zones parallel to the hexagonal prism a*. Photomicrograph by K. Schmetzer; immersion.*

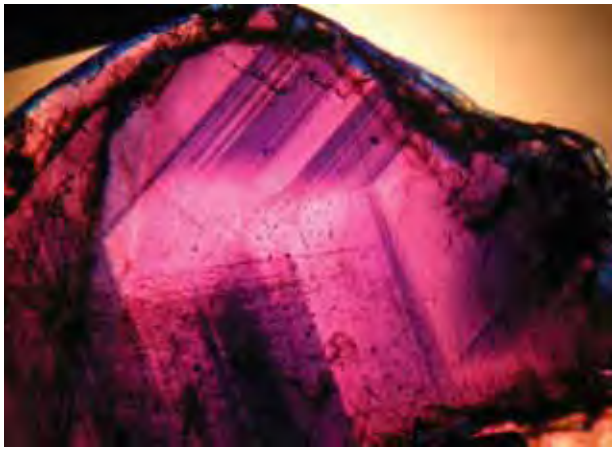

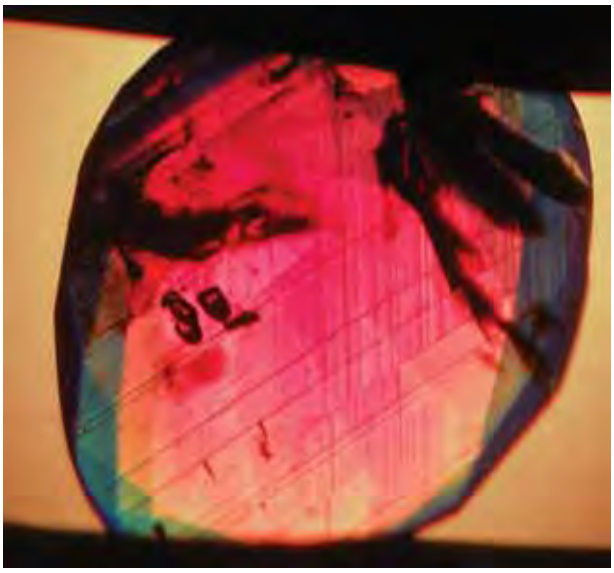

Figure 18. In this view perpendicular to the c-axis (which is horizontal) of a pink sample with layers of varying color intensity, growth patterns with color zoning are seen parallel to c *and* r*. Photomicrograph by K. Schmetzer; immersion, magnified 50×.*

pattern observed in rubies from Mong Hsu, Myanmar. To investigate whether such color zoning might be helpful for origin determination, as well as for separating faceted rubies and sapphires from their synthetic counterparts, the authors examined several samples of ruby and pink, pinkish orange, or pinkish

Figure 20. This sample shows complex color zoning, with bluish violet lamellae oriented parallel to the rhombohedra r *and* s*, and also parallel to various hexagonal dipyramids* n*. Photomicrograph by K. Schmetzer; immersion, magnified 50× and viewed approximately parallel to the c-axis.*

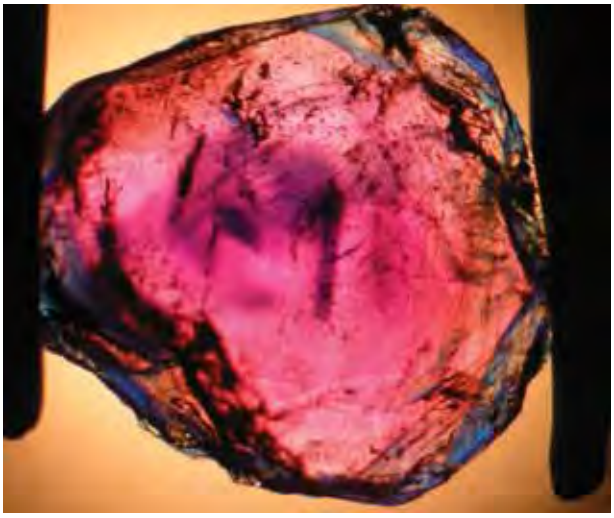

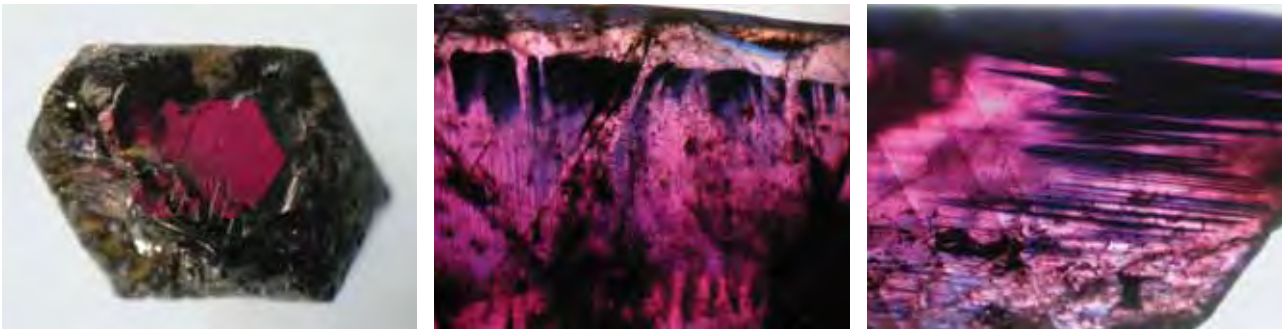

Figure 21. Viewed parallel to the c-axis, the 7-mm-wide dipyramidal corundum crystal on the left has a ruby core and a dark violetish blue (nearly black) rim. When another dipyramidal sample (center) is viewed perpendicular to the c-axis (which is horizontal in this photo), the bluish violet areas are restricted to small zones close to the rim. The rhombohedral sample on the right, which is also seen perpendicular to the c-axis (vertical in this photo), has bluish violet zones that appear as thin layers parallel to the basal pinacoid c. *Photomicrographs by K. Schmetzer; center and right taken in immersion, magnified 50×.*

violet sapphire with dark bluish violet- to black-appearing color variations (e.g., figure 22). Three different phases were identified:

1. Sapphire, which was black in reflected and transmitted light, but appeared bluish violet in thin slices or fragments (as described above).
2. Amphibole inclusions, which were black in reflected and transmitted light, but appeared green in thin areas. Such inclusions never revealed a fine lamellar or oriented pattern.
3. Black spinel rims on rubies with dipyramidal habit, but no black spinel was seen within the corundum crystals. Three chemical analyses gave a compositional range of $Mg_{0.5–0.6}Fe_{0.4–0.5}Al_2O_4$, which is intermediate between magnesium spinel and hercynite. Such rims are normally removed during the faceting process.

It was not always possible to distinguish between these three black-appearing phases without a detailed phase determination.

Twinning and Milky Domains. Rhombohedral twin planes (figure 23) were common. The samples typically contained one system of "intersection tubules," but three-dimensional arrangements of these tubules were also observed (figure 24).

Very common in the sapphires were slightly milky domains in the form of clouds, bands, or "growth sectors" (figure 25). In general, their milky appearance was caused by the presence of very tiny gray pinpoint inclusions.

Inclusions. *Elongate Needles.* The most distinctive features observed in Winza rubies were long tube-, fiber-, needle-, or hair-like inclusions (figure 26). These inclusions were especially common in the top-quality Winza rubies. The curved tubes were not observed in pink, purple, or blue samples. They were straight, slightly curved, bent, or even (rarely) spiral-like. They were filled with an orange-brown (probably polycrystalline) solid material, which generally did not give any useful signals when analyzed by Raman spectroscopy. A very large, slightly flattened tube exposed at the surface of a 0.60 ct faceted stone, however, showed an interesting mineral association. Several reflective (probably "unaltered") sections of the tube provided a clear amphibole

Figure 22. These corundum crystals have dark bluish violet- to black-appearing translucent to opaque phases exposed at their surfaces. The dark areas in the two crystals on the left were found to be blue-violet sapphire, the sample in the center (9 × 12 mm) contained black amphibole, and the two samples on the right had a rim of black spinel. Photo by K. Schmetzer.

Figure 23. Rhombohedral twin planes are common in Winza sapphires. Photomicrograph by V. Pardieu/GGL; magnified 40×, crossed polarizers.

Figure 24. Intersections of the twin lamellae resulted in the formation of linear tubules—typically one system, but also three-dimensional networks as seen here. Photomicrograph by V. Pardieu/GGL; magnified 30×.

Raman spectrum, while brownish material between the reflective areas was identified as hematite.

Mineral Inclusions. Mineral inclusions were quite common. Compared to rubies/sapphires from many other localities, however, we identified (by Raman analysis or electron microprobe) only a small variety of mineral species in our samples: amphibole, garnet, apatite, and spinel.

By far the most common inclusion mineral observed was amphibole. It was very typical in the sapphires, but observed in only one (top-quality) ruby. The amphibole inclusions showed large variations in color, size, and shape. Many amphibole crystals were nearly colorless, while others were slightly green to dark green or brownish green to nearly black, and often showed strong pleochroism. For the most part, the amphiboles displayed irregular, slightly rounded forms, but well-developed prismatic crystals also were common (figure 27). They occurred as single crystals or were clustered in groups or compact agglomerations. In some cases, they were accompanied by stress fissures in the host corundum.

The garnets were intense orange-yellow (figure 28); they were typically transparent and had well-developed or resorbed forms. Apatite was a very rare inclusion mineral (identified only in two of the top-quality rubies). It formed as colorless, transparent, prismatic, euhedral crystals that were not oriented crystallographically (figure 29). Spinel (Fe- and Mg-rich) was identified by electron microprobe as small inclusions in corundum, but it was not seen during

Figure 25. Winza sapphires commonly contain slightly milky domains caused by the presence of minute gray pinpoint inclusions. Photomicrograph by V. Pardieu/GGL; magnified 20×, fiber-optic illumination.

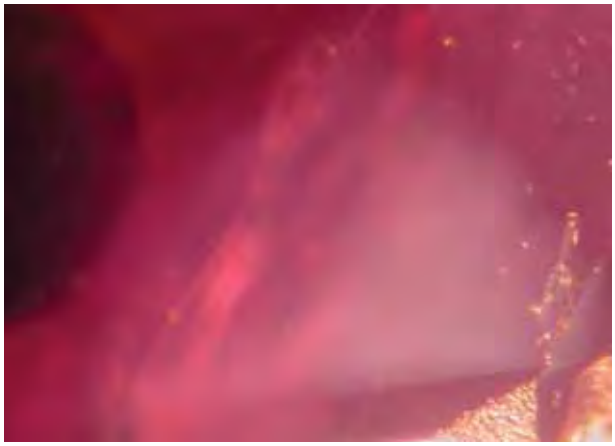

Figure 26. Probably the most characteristic features observed in some of the Winza rubies are long tube-, fiber-, needle-, or hair-like inclusions. These inclusions were especially common in the top-quality stones. Photomicrograph by V. Pardieu/GGL; magnified 40×.

Figure 27. Well-developed prismatic amphibole crystals are common in Winza corundum. The amphiboles do not show any preferred orientation in the corundum host; they can be considered as protogenetic inclusions. Photomicrograph by V. Pardieu/GGL; magnified 40×.

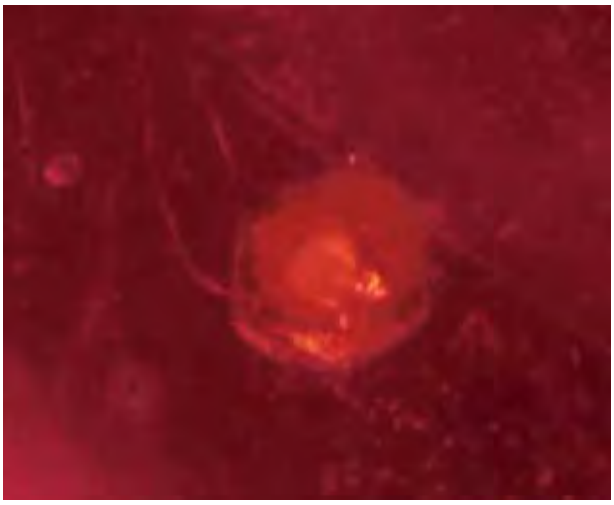

Figure 28. A well-formed orange-yellow garnet inclusion is present in this Winza ruby. Photomicrograph by V. Pardieu/GGL; magnified 40×.

the microscopic examination of the samples. It also formed dark rims surrounding dipyramidal rubies (see above). Opaque mineral grains displaying a grayish black metallic luster were tentatively identified as chalcocite (Cu_2S) by Raman analysis.

Uncommon in the sapphires were reflective particles that were generally accompanied by small, delicate, disk-like inclusions resembling the "thin films" more typical of basalt-related rubies (figure 30, left). Somewhat coarser particles were present in diffuse clouds or in stringer-like formations (figure 30, right).

Very rare were so-called comet tails associated with mineral inclusions (figure 31).

FTIR spectroscopy revealed the presence of various OH-bearing minerals, such as kaolinite, "limonite," chlorite, and (very rarely) boehmite. These were observed on fissure planes and as components of the

Figure 29. Colorless transparent apatite crystals were seen in only two Winza rubies. Photomicrograph by V. Pardieu/GGL; magnified 40×.

Figure 30. Minute oriented reflective particles were seen in a few samples, generally accompanied by small disk-like inclusions reminiscent of "thin films" (left, magnified 30×). Less common are coarser particles present in diffuse clouds or stringer-like formations (right, magnified 80×). Photomicrographs by V. Pardieu/GGL; fiber-optic illumination.

Figure 31. A group of mineral inclusions (probably amphibole) is accompanied by a weakly developed "comet tail" in this Winza sapphire. Note also the pink-blue color zoning and (slightly diffuse) fine light blue growth bands. Photomicrograph by V. Pardieu/GGL; magnified 40×, fiber-optic illumination.

tube fillings. They also may be present in the form of submicroscopic "particles."

Fractures and Fluid Inclusions. Unhealed fissures were quite common in the commercial-quality material. These fissures were either strongly reflective (mirror-like) or they displayed a slightly frosted appearance caused by the presence of a gray or brown substance (e.g., oxihydrates, identified by FTIR).

Partially healed fissures were often present in medium- to low-quality rubies/sapphires. In general, they showed relatively coarse textures with highly reflective inclusions that were rounded or irregularly shaped; well-developed networks or fingerprint-like patterns were rare. Less common were healed fissures composed of cavities that for the most part were developed as negative crystals containing polyphase fillings with black (opaque), brown, and colorless (transparent, singly and doubly refractive) constituents (figure 32) that could not be identified by Raman analysis.

Many fissures appeared to be filled with a grayish white or pale yellow solid material (figure 33) that could not be identified. These inclusions may resemble the flux material common in some synthetic rubies.

CHEMICAL COMPOSITION

EDXRF analyses revealed that Winza rubies and sapphires showed a relatively uniform chemical composition. The chromophores Cr and Fe were present in significant concentrations. Cr concentrations fell into the common range for rubies (including the pinkish red and purplish red material) originating from most occurrences: ~0.10–0.60 wt.% Cr_2O_3. For the blue to purplish blue sapphires, Cr_2O_3 ranged from ~0.10 to 0.30 wt.%.

The Fe concentration in the rubies was relatively high, with more than 95% of the samples in the range of ~0.30–0.80 wt.% Fe_2O_3. In very few samples, Fe_2O_3 reached up to ~1 wt.%. Top-color Winza rubies were characterized by a combination of relatively low Fe_2O_3 (~0.30–0.40 wt.%) and relatively high Cr_2O_3 (~0.40–0.60 wt.%). Blue to purplish blue Winza sapphires had Fe_2O_3 concentrations of ~0.60–0.95 wt.%.

Winza rubies of the best color contained very little or no Ti (typically below the detection limit). For the other samples, TiO_2 concentrations were ~0.005–0.020 wt.%. The blue to purplish blue Winza sapphires typically contained ~0.01–0.03 wt.% TiO_2; the highest value found was ~0.045 wt.% TiO_2.

The V concentration of the rubies and sapphires was generally low, and in many samples it was below the detection limit of ~0.005 wt.% V_2O_3. Most common were V_2O_3 contents in the range of ~0.005–0.015

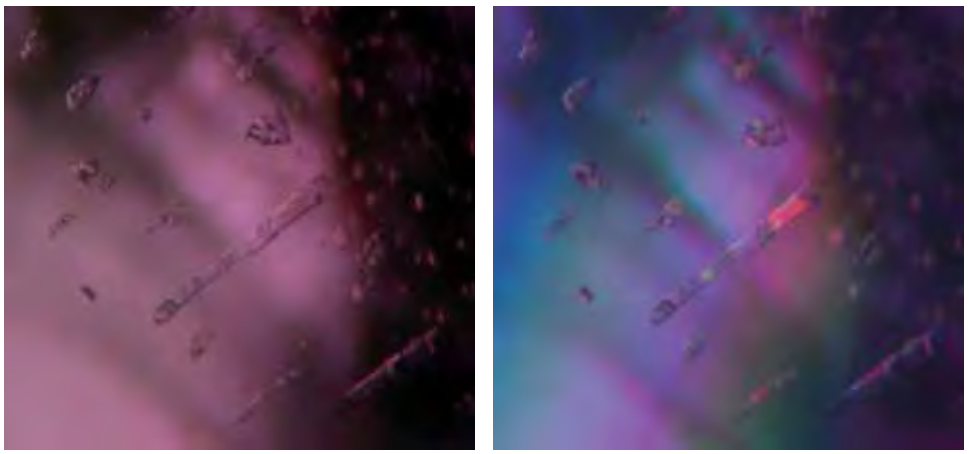

Figure 32. Partially healed fissures in some Winza rubies and sapphires were composed of negative crystals containing multiphase fillings with black-opaque and colorless-transparent (singly and doubly refractive) constituents. Photomicrographs by V. Pardieu/GGL; magnified 60×, brightfield (left) and cross-polarized (right) illumination.

Figure 33. These irregularly shaped cavities are filled with a grayish white to pale yellow solid substance. Such inclusions may resemble the flux material observed in synthetic gems. Photomicrograph by V. Pardieu/GGL; magnified 60×.

TABLE 4. Electron microprobe analyses of two samples of pale pink Winza corundum.

Oxide (wt.%)	Wz1_Cor[a]	Wz2_Cor[b]
Al_2O_3	98.80 ± 0.44	98.50 ± 0.18
Cr_2O_3	0.07 ± 0.02	0.05 ± 0.02
Fe_2O_3	0.36 ± 0.06	0.39 ± 0.06
TiO_2	0.02 ± 0.02	0.09 ± 0.08
Total	99.25	99.03

[a] *15 point analyses.*
[b] *6 point analyses.*

wt.%; rarely, values up to ~0.02 wt.% were measured.

Ga content, for the most part, was below the detection limit (~0.005 wt.% Ga_2O_3). The highest Ga concentration found was ~0.01 wt.% Ga_2O_3.

Electron microprobe analyses of two pale pink corundum crystals in a rock thin section showed appreciable Fe and significant Cr, along with traces of Ti (table 4).

TABLE 5. Chemical composition by LA-ICP-MS of different colors of gem corundum from Winza, Tanzania (in ppmw).[a]

Element	Red	N	Purple	N	Orange	N	Blue	N	Colorless	N
B	1.6 ± 1.7	26	1.9 ± 2.2	64	1.7 ± 1.3	32	3.8 ± 3.4	17	1.5 ± 0.8	34
Na	3.1 ± 8.1	40	4.7 ± 18	68	5.0 ± 19	37	2.5 ± 5.5	15	0.88 ± 2.4	23
Mg	39 ± 36	54	39 ± 33	120	36 ± 20	59	45 ± 36	30	26 ± 25	55
Al	519900 ± 2220	54	521300 ± 2090	120	521500 ± 2190	59	519500 ± 1640	30	521900 ± 1680	55
Si	4500 ± 1210	54	4060 ± 1650	120	3910 ± 1450	59	4710 ± 1180	30	3650 ± 830	55
P	21 ± 13	51	21 ± 13	110	17 ± 12	54	27 ± 14	24	14 ± 6.6	50
K	9.3 ± 8.8	12	16 ± 8.9	13	12 ± 16	7	7.8 ± 7.2	3	11 ± 7.5	3
Ca	38 ± 7	3	91 ± 56	5	42 ± 22	7	<40	0	25	1
Sc	0.060 ± 0.0025	2	0.10 ± 0.083	6	0.071 ± 0.025	6	<0.12	0	0.060	1
Ti	63 ± 63	51	120 ± 170	110	88 ± 110	56	280 ± 380	30	61 ± 64	55
V	2.5 ± 2	54	2.1 ± 1.4	120	2.1 ± 1.5	59	3.1 ± 1	30	1.8 ± 1.3	55
Cr	2350 ± 960	54	1390 ± 640	120	1310 ± 700	59	820 ± 270	30	520 ± 270	55
Mn	1.8 ± 2.6	10	3.9 ± 6.2	17	3.0 ± 5.8	7	3.2 ± 4.8	3	0.35 ± 0.2	2
Fe	2370 ± 670	54	2370 ± 590	120	2430 ± 670	59	3890 ± 990	30	3070 ± 890	55
Co	0.072 ± 0.053	19	0.068 ± 0.058	40	0.035 ± 0.023	24	0.056 ± 0.013	8	0.036 ± 0.018	15
Ni	3.3 ± 3.8	27	2.8 ± 2.1	67	2.4 ± 1.8	38	4.3 ± 1.8	14	1.8 ± 1.4	31
Cu	0.71 ± 0.98	20	8.2 ± 30	38	1.5 ± 2.7	14	7.4 ± 13	18	0.8 ± 2.2	20
Zn	2.8 ± 0.87	3	3.7 ± 2.4	5	1.7	1	<1.7	0	1.5	1
Ga	21 ± 6.5	54	25 ± 11	120	23 ± 6.6	59	28 ± 5	30	21 ± 7.7	55
Rb	0.034 ± 0.033	10	0.081 ± 0.078	12	0.11 ± 0.12	8	0.094 ± 0.13	3	0.034 ± 0.048	4
Sr	0.94 ± 2.4	13	3.0 ± 11	20	2.8 ± 6.6	8	1.0 ± 2.1	5	0.017 ± 0.0085	3
Zr	0.019 ± 0.004	6	0.29 ± 0.29	6	0.023 ± 0.011	2	0.17 ± 0.016	3	0.018	1
Nb	0.11 ± 0.16	10	0.057 ± 0.053	29	0.025 ± 0.022	13	0.034 ± 0.018	8	0.046 ± 0.034	5
Sn	0.22 ± 0.13	41	0.21 ± 0.13	81	0.25 ± 0.15	40	0.38 ± 0.12	21	0.21 ± 0.14	34
Cs	0.016 ± 0.019	3	0.11 ± 0.22	6	0.03 ± 0.016	4	0.020 ± 0.008	2	0.005 ± 0.001	2
Ba	1.4 ± 3.5	11	3.5 ± 8.5	12	4.1 ± 6.1	4	0.86 ± 1.3	4	0.097 ± 0.051	2
Ce	0.026 ± 0.017	8	0.088 ± 0.12	12	0.084 ± 0.076	4	0.12 ±0.066	6	0.013	1
Ta	0.078 ± 0.13	15	0.15 ± 0.2	30	0.046 ± 0.032	20	0.085 ± 0.063	9	0.18 ± 0.13	6
W	3.6 ± 7.8	28	2.2 ± 6.7	35	1.7 ± 3.4	23	0.35 ± 0.43	7	0.47 ± 0.89	7
Pb	0.20 ± 0.61	30	0.29 ± 0.77	66	0.16 ± 0.34	26	0.30 ± 0.38	18	0.10 ± 0.14	35

[a] *Notes: ppmw = parts per million by weight; < = value below the detection limit; N = number of values above the detection limit. Ablated material was carried to the ICP by He (5.0) carrier gas at a rate of 0.8 liters/minute (l/min). The plasma conditions of the ICP-MS were optimized to maximum intensity at U/Th ratio ~1 and Th/ThO ratio <0.5. This was achieved using the following parameters: plasma gas flow (Ar) 14.0 l/min, nebulizer gas flow (Ar) 0.85-0.9 l/min, auxiliary gas flow (He) 0.70–0.75 l/min, and RF power 1400 W. In the corundum matrices, the elements Be, B, Na, Mg, Al, Si, P, K, Sc, Ti, V, Cr, Mn, Fe, Co, Ni, Cu, Zn, Ga, Rb, Sr, Zr, Nb, Mo, Sn, Cs, Ba, Ce, Ta, W, Pb, Th, and U were measured quasi-simultaneously in each individual analysis.*

LA-ICP-MS data for Winza corundum are reported in table 5. Generally, Si, Cr, and Fe were abundant, with concentrations above 500 ppm (0.05 wt.%). Traces of B, Na, Mg, P, Ti, V, Co, Ni, Cu, Ga, Sn, Ta, W, and Pb were commonly present. Na, Mg, Ti, Cr, V, and Fe were variable, while all other elements occurred in quite constant concentrations. A weak positive correlation was observed for the elements V and Ti.

SPECTROSCOPY

UV-Vis-NIR spectroscopy of Winza rubies revealed the well-known Cr^{3+} absorption bands at ~405–410 and 560 nm (figure 34, top). In addition, the spectra generally displayed a strong "background absorption" starting around 600 nm and increasing toward the UV edge. The absorption spectra of blue to purple-blue and padparadscha sapphires were, in general, combination spectra showing the Cr^{3+} absorption features together with a pronounced contribution of Fe^{3+} bands at 377/388 nm and 450 nm (figure 34, middle). More rarely seen was a combination of the Cr^{3+} features with the Fe^{2+}-Ti^{4+} charge-transfer band of sapphire at around 700 nm (figure 34, bottom). The Cr "doublet" at 694 nm was visible in all spectra.

The FTIR spectra in the mid-infrared region between 5000 and 1500 cm^{-1} allow for the distinction of four main features (figure 35):

1. A more-or-less pronounced broad band with a maximum at ~3450 cm^{-1} was recorded in 41 of the 59 samples tested (spectrum A).
2. A prominent peak at ~3160 cm^{-1}—with accompanying peaks at ~3350, 3240, and 2420 cm^{-1}—was recognized in 38 samples (spectrum B). Most of the remaining samples showed a shoulder (sometimes very weak) at 3160 cm^{-1}. The 3160 cm^{-1} absorption was completely absent from only a very few samples. It is interesting to note that the "3160 group" (also named "3161-series"; Smith and Van der Bogert, 2006) was most prominent in the high-quality Winza rubies (i.e., in more than 90% of these stones).
3. An additional group of absorption peaks at ~3695, 3670, 3650, and 3620 cm^{-1} was rarely exhibited by high-quality rubies (spectrum C).
4. Distinct band groups in the 3560–3420 cm^{-1} region were detected in only three samples (spectrum D).

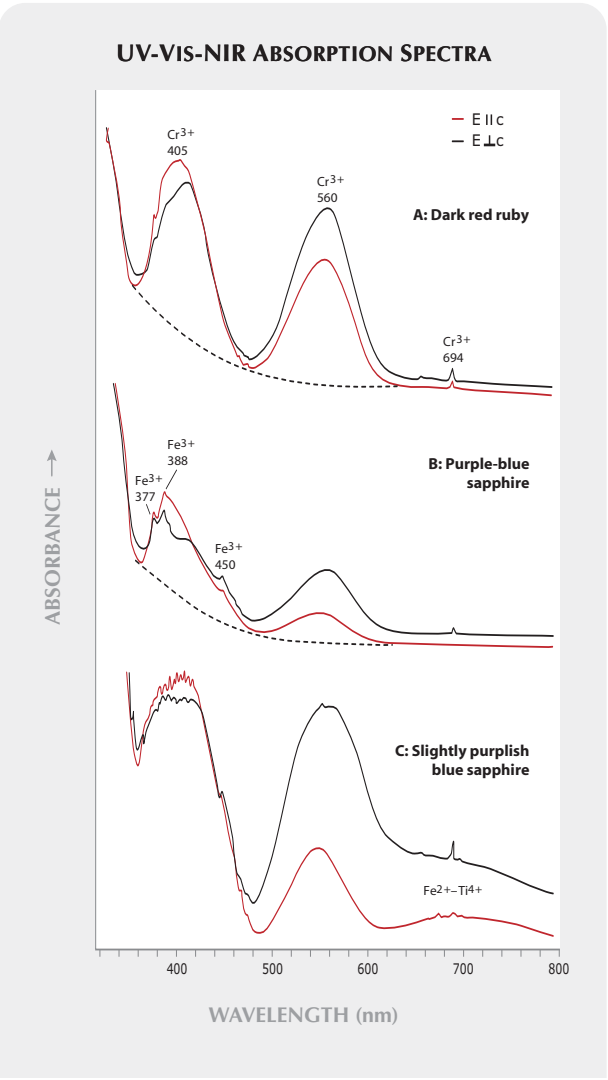

Figure 34. Polarized UV-Vis-NIR absorption spectra of Winza rubies show typical Cr^{3+} absorption bands at ~405–410 and 560 nm, as well as a strong "background absorption" (dotted line) in the UV region (A). The absorption spectra of blue to purple-blue sapphires from Winza generally show a combination of Cr^{3+} absorption features together with Fe^{3+} bands at 377/388 nm and 450 nm (B). Less common are combinations of the Cr^{3+} features with a Fe^{2+}-Ti^{4+} charge-transfer band at ~700 nm (C, from a slightly purplish blue Winza sapphire).

The spectral features described above may be present in combination, with varying intensities of the different components (see, e.g., the combination of the band groups in the 3560–3420 cm^{-1} region and the 3160 cm^{-1} absorption in spectrum E, observed in a top-quality ruby). In two samples, weak peaks related to boehmite were detected at around 2100 and 1980 cm^{-1} (e.g., spectrum A).

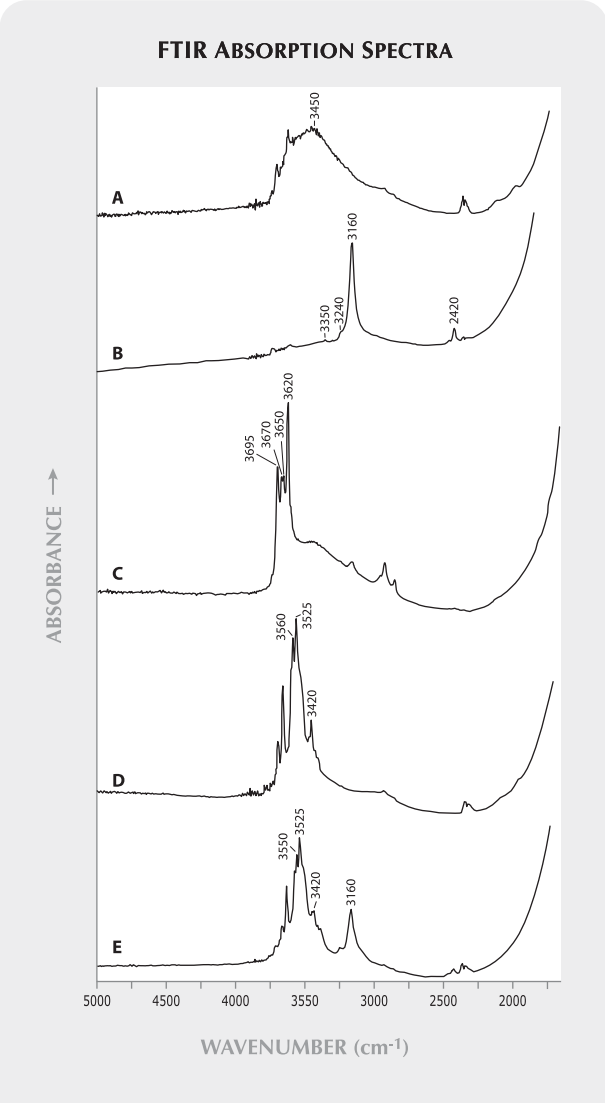

Figure 35. Unpolarized IR absorption spectra of Winza rubies showed four main features in the mid-infrared region between 5000 and 1500 cm^{-1}: (A) a broad band at ~3450 cm^{-1}; (B) a prominent peak at ~3160 cm^{-1} often accompanied by peaks at ~3350, 3240, and 2420 cm^{-1}; (C) a group of absorption peaks at ~3695, 3670, 3650, and 3620 cm^{-1}; and (D) distinct bands in the 3560–3420 cm^{-1} region. These features may be present in combination and with varying intensities, as in spectrum E. In two samples, weak peaks related to boehmite were detected at around 2100 and 1980 cm^{-1} (e.g., spectrum A). Features seen at 2917, 2853, and 2349 cm^{-1} were caused by sample contamination.

OXYGEN ISOTOPE COMPOSITION

The oxygen isotope compositions obtained for three Winza rubies were $\delta^{18}O$ = 4.6‰, 4.7‰, and 4.9‰ (figure 36), giving a mean $\delta^{18}O$ of 4.7 ± 0.15‰. For information about the use of oxygen isotopes to characterize corundum from different deposits, see Giuliani et al. (2007).

HEAT-TREATED SAMPLES

Heat-treated Winza rubies examined by one of the authors (DS) in Bangkok in May 2008 showed a distinct orangy red hue (as seen in the sample on the left in figure 16). The most striking internal feature was the presence of partially healed fissures displaying strong alteration patterns, with a drop-like or network-like melting appearance that is typical of intensely heat-treated rubies/sapphires. In part, these partially healed fissures were associated with altered mineral inclusions. Identical features were observed in the heat-treated rubies submitted to GGL for testing in Hong Kong in September 2008. The infrared spectra recorded for these samples did not show any features related to the presence of OH/H_2O (see Discussion below).

Comparison of the three pairs of unheated/heated corundum showed that the orangy red sample did not change color. However, one of the purplish pink samples became intense red-orange after heat treatment. The second purplish pink sample developed an inhomogeneous color distribution, with orange and violet areas. All the unheated pieces showed the 3160 cm^{-1} absorption in varying intensity; these bands disappeared from the heat-treated samples.

DISCUSSION

Physical Properties. The measured refractive indices and specific gravity values from Winza (table 3) are consistent with those known for rubies and sapphires from all other localities. The morphology of the crystals is quite variable, and some of the samples have habits not seen previously in material from other ruby/sapphire deposits.

Microscopic Characteristics. *Growth Features and Color Zoning.* Although some Winza material may bear a superficial resemblance to Mong Hsu rubies, the orientation of the thin bluish violet lamellae within Winza corundum is completely different. Mong Hsu rubies typically have dark cores that are formed by bluish violet layers oriented parallel to rhombohedral and dipyramidal faces (Peretti et al., 1995). In the Winza samples, the bluish violet color zoning was oriented parallel to the prism and basal pinacoid, occasionally in combination with bluish violet layers oriented parallel to rhombohedral and dipyramidal faces. Such zoning has not been

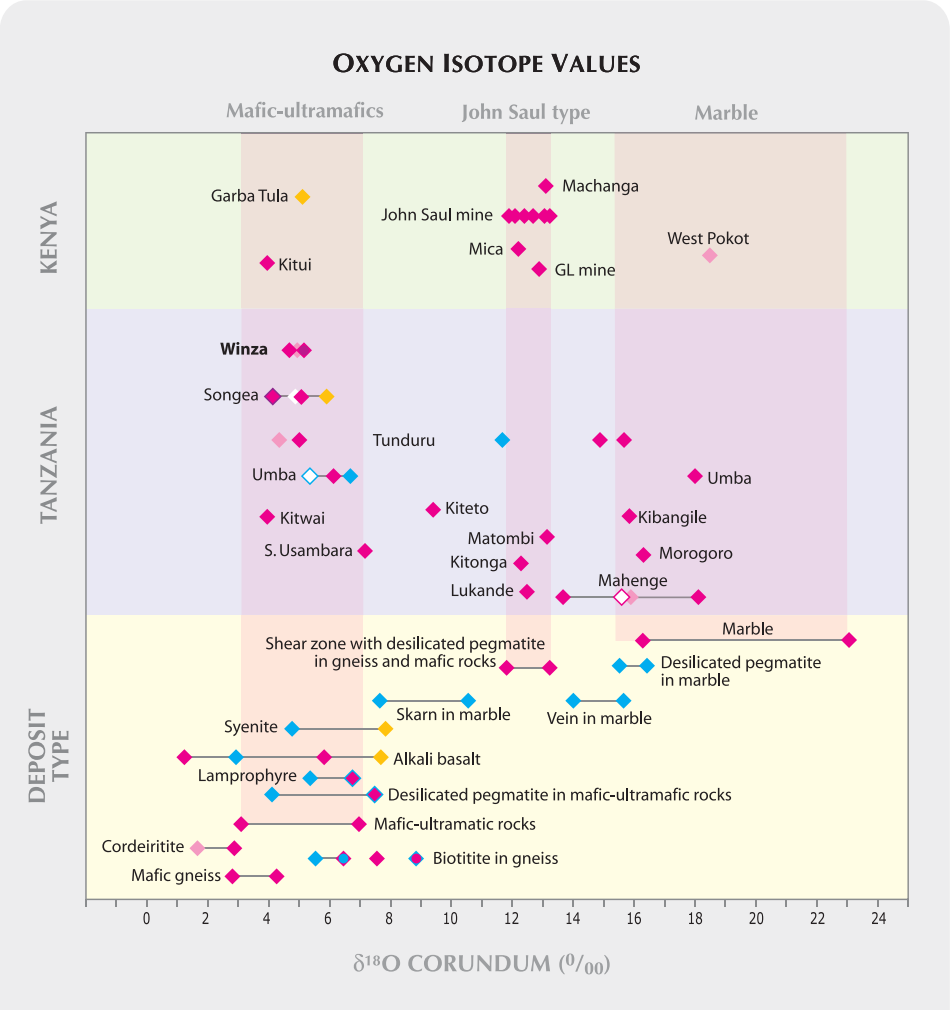

Figure 36. Oxygen isotope values for three rubies from Winza are shown with those for corundum from various types of primary and secondary deposits in Kenya and Tanzania. The data are reported in the conventional delta notation relative to V-SMOW (Vienna Standard Mean Ocean Water) equal to 0‰, and are compared with the oxygen isotopic ranges defined for various deposit types, after Giuliani et al. (2005, 2007). The symbol colors correspond to sample colors; white symbols represent colorless sapphires.

observed in gem corundum from other localities, to the best of the authors' knowledge.

Inclusions. Our findings are consistent with previous reports of inclusions in Winza corundum (Abduriyim and Kitawaki, 2008; GIT Gem Testing Laboratory, 2008; Hänni and Krzemnicki, 2008; Krzemnicki and Hänni, 2008; Pardieu and Schwarz, 2008; Smith et al., 2008).

Microscopic examination often can be used to distinguish Winza rubies/sapphires from those originating in other genetic environments or geographic localities. The following internal characteristics can be considered locality-specific for rubies/sapphires from Winza: (1) long tube-, fiber-, needle-, or hair-like inclusions of orange-brown color that are straight, slightly curved, bent, or rarely show a spiral-like appearance (restricted to medium red and vivid [orangy] red Winza rubies); and (2) a suite of mineral inclusions composed of amphibole + garnet + apatite + an opaque mineral (tentatively identified as chalcocite, based on Raman data); (3) any of various types of color zoning; (4) partially healed fissures composed of cavities displaying varying shapes (irregular, but also regular and developed as negative crystals) that contain a polyphase filling; (5) fissures containing a grayish white to pale yellow substance that often resembles flux residues in synthetic rubies; and (6) rhombohedral twin planes. The polyphase filling material of (4) shows various colors (black, brown, or colorless) and could not be identified. No Raman signal could be obtained for these fillers or those of (5).

The variety of mineral inclusions observed in Winza corundum is rather small compared to that seen in rubies and sapphires from other localities. The internal mineral association of a ruby or sapphire always reflects the nature of the host rock in which it crystallized. The association amphibole + garnet + plagioclase (+ kyanite identified as an accessory mineral) in the host rock indicates that the corundum formed in a metamorphic environment. Rubies from other localities reveal, in general, quite different

inclusion mineral associations (e.g., Henn et al., 1990; Hughes, 1997; Mercier et al., 1999; Simonet, 2000; Schwarz, 2001; and GGL database). Marble-hosted rubies from Myanmar's Mogok stone tract, for example, contain mostly rutile (needles and/or irregularly rounded opaque crystals of varying size), carbonates, sphene, zircon, apatite, garnet, graphite, spinel, sphalerite, pyrite, pyrrhotite, mica, olivine, pargasite, and anhydrite (the association "rutile + sphene + zircon" is probably locality-specific for rubies from Mogok).

Chemical Properties. SSEF (2008) reported Cr and Fe as the main trace elements, with "little" Ga, and Ti and V below the detection limit of their EDXRF instrument. Semiquantitative EDXRF analyses performed by GIT Gem Testing Laboratory (2008) indicated moderate contents of Cr (0.35–0.68 wt.% Cr_2O_3) and Fe (0.25–0.41 wt.% Fe_2O_3), very low to low amounts of Ti (55–192 ppm TiO_2) and V (from not detectable to 164 ppm V_2O_3), and low-to-moderate Ga contents (64–146 ppm Ga_2O_3). These values are in fairly good agreement with our data.

Comparison with Rubies from Different Genetic Environments. The chemical fingerprint of Winza rubies is quite different from that of rubies originating from marble-type deposits such as Mogok (figure 37A). The main difference is in the iron concentration: Rubies from marble host rocks typically have low iron contents. In Mogok and Mong Hsu rubies, for example, GGL data show that the Fe_2O_3 concentration is normally below ~0.05 wt.%. However, the lower Fe_2O_3 limit we found for Winza rubies is ~0.3 wt.%, and GIT Gem Testing Laboratory (2008) reported 0.25 wt.%. When comparing the Cr and Fe contents of Winza rubies with those of basalt-related rubies from the Thai/Cambodian border region, we found an almost complete overlap of the chemical data (see again figure 37A).

Comparison with Rubies Originating from Other African Deposits. Rubies from Songea, Tanzania, generally have low-to-moderate contents of Ti, V, and Ga—often below the EDXRF detection limit. The highest concentrations of these elements (from the analysis of ~30 samples; Schwarz, 2001) are ~0.03 wt.% TiO_2, 0.05 wt.% V_2O_3, and 0.05 wt.% Ga_2O_3. The Cr content of Songea rubies normally varies between ~0.2 and 0.7 wt.% Cr_2O_3 (as compared to ~0.1 wt.% to ~0.6 wt.% [occasionally ~0.8 wt.% for top-quality] for Winza rubies). Songea rubies distinguish themselves by very high Fe contents (this is valid for the entire Songea corundum production, independent of the bodycolor)—~0.8–2.0 wt.% Fe_2O_3—as compared to ~0.3–0.8 wt.% Fe_2O_3 for Winza rubies. As evident in figure 37B, there is minimal overlap between Songea and Winza in Cr and Fe.

Rubies from Kenya's Mangari region most commonly show ~0.005–0.15 wt.% Fe_2O_3 (very rarely up

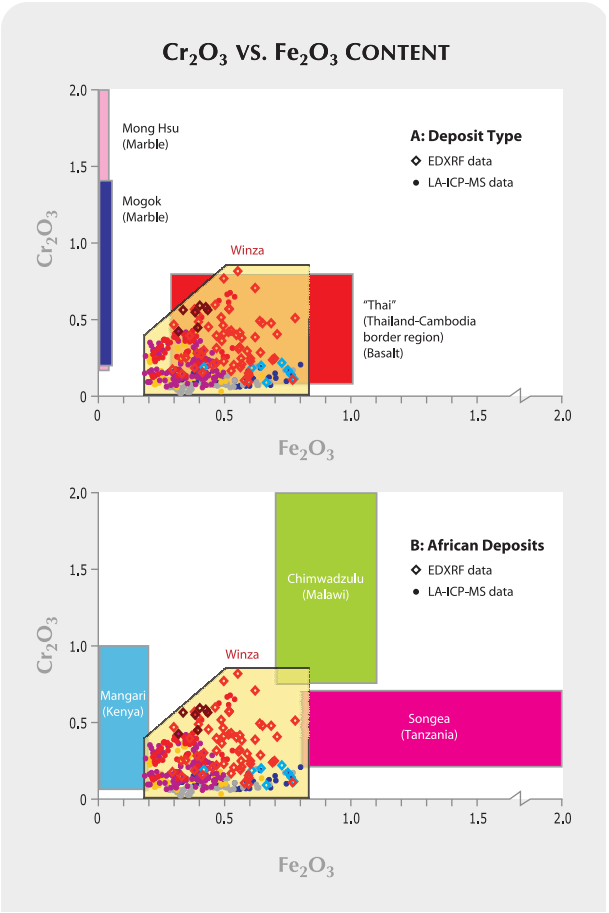

Figure 37. In a plot of Cr vs. Fe, more than 90% of the Winza rubies (red) and sapphires (other colors) fall into a population field extending from ~0.30 to 0.80 wt.% Fe_2O_3 and ~0.10 to 0.60 wt.% Cr_2O_3. Top-quality Winza rubies fall into the upper left area of this field, while blue to purplish blue Winza sapphires are located near the lower right corner. In plot A, marble-hosted rubies from Mogok and Mong Hsu largely overlap one another, but they are completely separate from Winza. However, there is extensive overlap between stones from Winza and those of basalt-related rubies from the Thai/Cambodian border region. In plot B, Malawi rubies are distinguished by relatively high Cr contents. Mangari rubies typically have low Fe (mostly, <0.05 wt.% Fe_2O_3, but they may attain 0.2 wt.% Fe_2O_3), while Malawi rubies vary from ~0.7 to 1.1 wt.% Fe_2O_3. The highest Fe concentrations were found in rubies from Songea: ~0.8–2.0 wt.% Fe_2O_3.

to ~0.2 wt.%). This range, too, only very slightly overlaps the Fe content of Winza rubies (again, see figure 37B). The Cr contents of Mangari rubies fall mostly into the range of ~0.3–1 wt.% Cr_2O_3, which does overlap those from Winza.

The Fe and Cr contents of Malawi rubies are also quite different from those of Winza (again, see figure 37B), despite the fact that there are some similarities in their host-rock composition (Fe/Cr-rich amphibolite; Dill, 2005). Rubies from the Chimwadzulu Hill deposit have somewhat higher Fe contents (~0.7–1.1 wt.% Fe_2O_3) and a distinctly higher Cr concentration (~0.75–2 wt.% Cr_2O_3). GGL data indicate that rubies from both deposits have low Ti (generally <0.03 wt.% TiO_2), V (normally <0.02 wt.% V_2O_3), and Ga (often below detection limit; highest concentration found was ~0.01 wt.% Ga_2O_3).

There is very little LA-ICP-MS data for gem corundum available in the literature for comparison. Rankin et al. (2003) reported concentration ranges of Mg, Ca, V, Cr, Fe, Cu, and Ga for rubies originating from Longido (Tanzania) and Chimwadzulu Hill. Winza rubies and sapphires have Mg, Cr, Fe, and Ga concentrations that are equal to or slightly lower than the element concentration ranges reported by Rankin et al. (2003). Calcium, V, and Cu are much lower in Winza rubies and sapphires compared to stones from Longido and Chimwadzulu Hill.

Spectroscopy. The GIT Gem Testing Laboratory (2008) reported that the UV-Vis absorption spectra of Winza rubies typically show the Cr^{3+} bands and lines together with Fe^{3+} absorptions (377/387 and 450 nm) that would be expected for a ruby with high iron content.

The dominant absorption feature in chromium-colored corundum is the presence of intense bands related to Cr^{3+} at 405 and 560 nm. Additional spectral features observed for rubies are: (1) the so-called "background absorption," which represents an increasing absorption toward the UV edge; and (2) the presence of Fe^{3+}-related groups at ~375 nm and 450 nm. Rubies with low Fe contents (e.g., marble-hosted Mogok rubies and most rubies from Kenya's Mangari region) typically show relatively "pure" Cr^{3+} spectra with variable, but low, UV absorption. The other "extreme" is provided by corundum from Songea. These rubies (and also sapphires of various colors) are characterized by very strong Fe^{3+}-related features (Schwarz, 2001). Rubies from Malawi show, in general, spectra with combined Cr^{3+}/Fe^{3+} absorption components.

Winza rubies and pink/purple sapphires, as well as rubies from the Thai/Cambodian border region, show the chromium bands and a generally strong "background absorption," which is influenced by several factors (figure 34A). Features related to Fe^{3+} are only weakly developed. Blue to purplish blue Winza sapphires display distinct Fe^{3+}-related features (figure 34B), or they show the combination of Cr^{3+} bands and the Fe^{2+}-Ti^{4+} charge-transfer absorption around 700 nm (figure 34C).

The padparadscha sapphire that was examined for this report owed its color to Cr^{3+}/Fe^{3+} absorptions, rather than the combination of Cr^{3+} and color centers that are seen in "classic" padparadscha sapphires (i.e., from Sri Lanka). GIT Gem Testing Laboratory (2008) described three diagnostic patterns for OH-related peaks in the mid-IR absorption spectra of Winza rubies: Pattern A showed a broad absorption band from 3735 to 3000 cm^{-1}, centered around 3450 cm^{-1}, assigned to goethite. Pattern B showed absorption bands with approximate peaks at 3335, 3242, 3160, 3075, 2459, and 2420 cm^{-1}. Pattern C showed mixed absorption bands from patterns A and B.

Smith and Van der Bogert (2006) commented on the 3161 cm^{-1} spectral feature (formerly described mainly in natural-color yellow sapphire from Sri Lanka). They indicated that, when present in high intensity, it appears to consist of at least six bands. This so-called 3161 series was attributed by past researchers to OH groups involved in charge-compensation with Si^{4+}. Smith and Van der Bogert (2006) suggested that the 3161 series is actually due to structurally bonded OH associated with Mg^{2+}. The average Mg contents measured in our samples were in the range of 30–65 ppm (table 5). The evaluation of whether this concentration is sufficient to support the "Mg-OH model" is beyond the scope of this article.

Balmer et al. (2006) reported that peaks at 3353 and 3242 cm^{-1} are probably associated with the 3160 cm^{-1} absorption. They could not confirm whether this group of peaks is related to goethite or to silanol groups (OH group attached to Si^{4+}).

The FTIR spectra of the present study allow the following correlations:

1. All top-quality rubies containing the orange-brown tube/hair-like inclusions had the 3160 cm^{-1} absorption as the dominant feature.
2. Only one sapphire showed a comparably prominent 3160 cm^{-1} feature.
3. The 3160 cm^{-1} absorption was present in almost all of the lower-quality samples, but it

appeared very weak or as a low shoulder when in combination with other bands.

4. Very few samples did *not* have the 3160 cm^{-1} feature.

These results imply that, although there is a strong correlation between the orange-brown tube/hair-like inclusions and a prominent 3160 cm^{-1} absorption, other factors must be taken into consideration. Since there is no clear correlation between other microscopic features and the presence/intensity of the 3160 cm^{-1} absorption band, the influence of submicroscopic inclusions should be considered.

The characteristic group of four peaks with maxima at 3695, 3670, 3650, and 3620 cm^{-1} (spectrum C in figure 35) is typically attributed to kaolinite minerals (Beran and Rossman, 2006). This group was found in 17 samples (in four top-quality rubies, this group was weak, while in other samples it was, in part, quite strong).

According to A. Beran (pers. comm., 2008), the broad 3450 cm^{-1} absorption band (spectrum A in figure 35) is related to H_2O (submicroscopic inclusions or adsorptive humidity).

OH bands associated with the presence of chlorite-group minerals show typical absorption features in the range between 3560 and 3420 cm^{-1} (spectrum D in figure 35).

Geologic Origin. Observations by two of the authors (VP and BML) of primary deposits at Winza, as well as the examination of corundum-bearing host-rock specimens in the laboratory, showed a close association between corundum and cross-cutting layers or "dikes" of a garnet-bearing amphibolitic rock. Macroscopic observations by authors GG and DO of a sample obtained by JMS (figure 9) clearly showed that, according to its mineralogy, the dike-like body was mafic in composition before it was metamorphosed. Possible lithologies for the protolith include high-alumina gabbros (layered gabbros) or leucogabbros. The central part of the "dike" is composed of a metamorphic garnet + hornblende ± plagioclase ± corundum association. Metamorphic conditions estimated by using garnet-amphibole-corundum equilibria (winTWQ; Berman, 2007) showed that the metamorphic overprint was 800 ± 50°C and 8–10 kbar.

The color/growth zones of the corundum are commonly complex, which indicates crystal development during a number of stages characterized by variable Ti, Cr, and Fe availability.

Spinel that (rarely) overgrows or is included in the corundum is Fe- and Mg-rich, whereas spinel from the host amphibole is Cr-rich, with up to 32 wt.% Cr_2O_3 (unpublished electron microprobe data of the authors). The presence of two chemically distinct spinel compositions indicates that two different generations are present. The Cr-spinel is probably a relict of the initial magmatic rock before the metamorphism, while the Fe- and Mg-rich spinel crystallized during the metamorphic stage that formed the corundum.

The amphiboles did not show any preferred orientation in the host corundum; they can be considered protogenetic inclusions reflecting the nature of the host rock. Amphibole inclusions showing various morphologies were commonly present. This is a strong indication that *all* the corundum morphologies originated from an amphibolite environment.

In the ternary Mg-Fe-Ti diagram that was established by Peucat et al. (2007) to distinguish magmatic from metamorphic sapphires, the chemical fingerprint of the Winza sapphires overlaps the border separating the metamorphic and magmatic population fields (figure 38).

Oxygen isotope values for three Winza corundum samples defined a consistent and restricted $\delta^{18}O$ range of 4.7 ± 0.15‰, indicating that they formed under comparable genetic conditions. This composition suggests two possible origins for Winza rubies (Giuliani et al., 2005, 2007): either in metamorphosed mafic-ultramafic rocks (worldwide $\delta^{18}O$ range of 3.2–6.8‰, n = 19), or in desilicated pegmatites within mafic-ultramafic rocks such as plumasites (4.2–6.7‰, n=16). We therefore conclude that the Winza rubies are of metamorphic origin, with a high-alumina meta-(leuco)gabbro as the protolith for the host rock.

Formation of the rhombohedral top-quality rubies with their exceptional combination of large size, intense color, and high transparency requires growth conditions different from those of the lower-quality corundum (characterized by a prismatic-tabular or dipyramidal morphology and the general presence of strong color zoning and abundant inclusions that reduce their transparency). An explanation for the (co-)existence of these two corundum types in the Winza area could be that they represent separate corundum "generations" formed at different geologic times or under locally different pressure-temperature (PT) conditions.

Separation from Synthetics and Heat-treated Natural Corundum from Other Sources. When the first Winza rubies appeared on the market, they were praised for

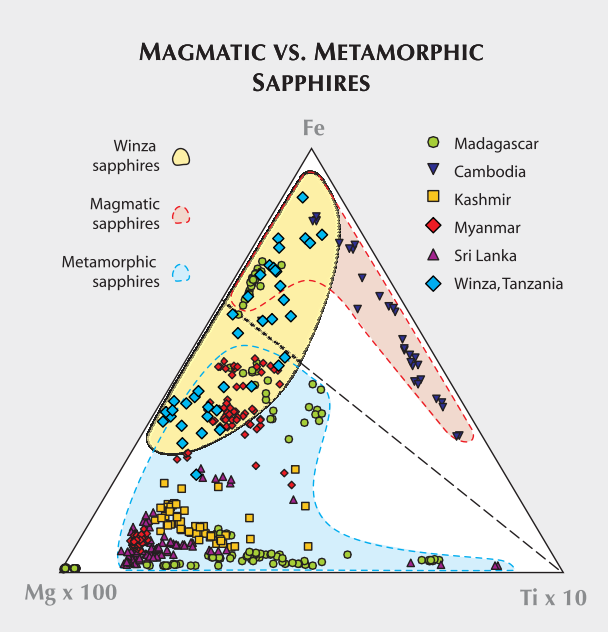

Figure 38. This ternary Fe-Mg-Ti diagram shows LA-ICP-MS data for blue sapphires originating from Winza and other deposits (all data points from GGL database). Peucat et al. (2007) defined two population fields for magmatic- and metamorphic-type blue sapphires. Note that the blue sapphires from Winza plot in a range overlapping both fields (this could indicate that melting processes might be involved, related to high-PT metamorphism). Modified from Peucat et al. (2007).

their exceptional color and clarity. At the same time, they caused suspicion and doubt, because the top-quality stones possessed such a high transparency and bright color that many dealers and gemologists who saw them for the first time thought they were synthetic. The identification and separation of Winza rubies from synthetics is generally quite easy—as long as the typical internal features described above are present. These are mineral inclusions such as amphibole, garnet, and apatite; orange-brown "tubes/needles/hairs"; and color zoning in various patterns. Only one inclusion feature could potentially cause confusion: Partially healed fissures consisting of irregularly shaped cavities filled with a grayish white to pale yellow solid material may resemble the flux components seen in some synthetics.

Another powerful tool for the separation of Winza rubies from synthetics (especially if characteristic inclusions are not present) is chemical fingerprinting, notably the Cr/Fe correlation. Elements such as Ti, V, and Ga are of little help because their contents are normally quite low in synthetic rubies/sapphires, as they are in the stones from Winza. The key element for the separation is Fe: Contents in the range of ~0.3 to 0.8 wt.% Fe_2O_3—which are typical of rubies/sapphires from Winza—are only rarely found in synthetic rubies. "High-iron" synthetic rubies are known from Douros (flux grown), Ramaura (flux grown), Gilson (flux grown), and Tairus (hydrothermally grown). In a detailed study by Schwarz et al. (2000), however, only very few synthetic rubies were found with Fe_2O_3 contents reaching the lower limit of the Winza rubies. These included some hydrothermal synthetic rubies and a very few flux synthetics grown by Douros (2 out of 35) and from the (experimental) production of Gilson (2 out of 27). Gilson synthetic rubies have not been produced and marketed commercially. In addition, all the flux synthetic samples examined by one of the authors (DS) showed healed fissures with typical flux patterns. Douros samples also distinguish themselves by high Ga concentrations (~0.04 to 0.1 wt.% Ga_2O_3). Practically all production from Tairus shows diagnostic internal features (especially pronounced growth structures). Therefore, chemical fingerprinting, when applied with other standard gemological tests, is an effective method for the separation of Winza rubies from synthetics.

The same is valid for the separation of heat-treated Winza rubies/sapphires from stones of other sources. Since heat treatment results in the alteration of fissure textures and solid inclusions, it tends to remove locality-specific internal features. Chemical fingerprinting is not affected by traditional heat treatment and can, therefore, be used in the same way as described for unheated stones. We believe that probably less than 1% of the faceted gems from Winza now on the market have been heat treated. This percentage may increase in the future if treaters are successful in applying heating techniques to pink, purple, or pinkish and purplish red starting material.

SUMMARY AND CONCLUSION

The arrival on the market of very fine cut rubies (e.g., figure 39) from a new deposit near Winza in central Tanzania was welcomed by the international gem trade, as the supply of top-quality rubies is scarce. It is difficult to predict if Winza will become a major source of fine rubies. Only time will tell. But if the area consistently produces fine stones and if a market is found for the lower-quality material, this mining region could become more than a gem rush.

Winza rubies and sapphires are hosted by metamorphic rocks of the Usagaran Belt. Observations of the associated mineral assemblages indicate that

Figure 39. The Winza area of central Tanzania is a new source of fine untreated ruby, such as the 3.18 ct center stone in this ring. Courtesy of The Collector Fine Jewelry, Fallbrook, California; photo by Robert Weldon.

the gem corundum is metamorphic in origin. The corundum is contained in "dikes" consisting mainly of the assemblage amphibole-garnet ± plagioclase. Oxygen isotope data are consistent with an origin in metamorphosed mafic-ultramafic rocks.

The physical properties of Winza rubies and sapphires are quite constant, with RIs and SGs in the same range known for rubies and sapphires originating from other localities. However, Winza rubies and sapphires can be characterized by inclusion features that, in part, can be considered locality specific: long tube-, fiber-, needle-, or hair-like inclusions, containing an orange-brown, solid polycrystalline material (most likely limonite); amphibole crystals showing large variations in shape, along with garnet and possibly apatite and/or an opaque mineral; partially healed fissures containing cavities filled with a polyphase material; and fissures containing primarily a grayish white to pale yellow substance. These internal features provide confirmation of natural origin and are a very strong indication of the host stone's locality of origin. Only the fissures with the grayish white to pale yellow substance may cause confusion, because they can resemble flux material in synthetic corundum. The specific type of bluish violet color zoning seen in rhombohedral and dipyramidal samples has not been previously found in natural ruby or pink sapphire, to the best of our knowledge, so it is also useful for determining a Winza origin.

The chemical composition of Winza rubies and sapphires, which formed in association with amphibolites, is characterized by a relatively high Fe content. This separates them from most natural and almost all synthetic counterparts. Although there is extensive chemical overlap with rubies originating from the Thai/Cambodian border region, the latter display internal features that are totally different from the inclusions in Winza stones.

ABOUT THE AUTHORS

Dr. Schwarz (d.schwarz@gubelingemlab.ch) is research manager, Dr. Klemm is analyst, and Ms. Malsy and Dr. Erel are gemologists, at the Gübelin Gem Lab, Lucerne, Switzerland. Mr. Pardieu was a gemologist at the Gübelin Gem Lab at the time this article was prepared, and is now field gemologist at the GIA Laboratory in Bangkok. Dr. Saul is an independent geologist based in Paris. Dr. Schmetzer is a research gemologist residing in Petershausen, Germany. Mr. Laurs is editor of Gems & Gemology *at GIA in Carlsbad, California. Dr. Giuliani is senior researcher in geology at the IRD (Institut de Recherche pour le Développement) and CRPG/CNRS, Nancy, France. Dr. Hauzenberger is associate professor of mineralogy and petrology at the Institute of Earth Sciences, University of Graz, Austria. Mr. Du Toit is manager of the Gemstone Identification Department at the GIA Laboratory in Bangkok. Dr. Fallick is geochemist at the Isotope Geosciences Unit, Scottish Universities Environmental Research Centre, Glasgow, Scotland. Dr. Ohnenstetter is petrologist at CRPG/CNRS.*

ACKNOWLEDGMENTS

Mark and Eric Saul (Swala Gem Traders Ltd., Arusha, Tanzania), Jean Baptiste Senoble (Nomads Ltd., Bangkok), and Abdul Msellem (Arusha) are thanked for providing support during author VP's visit to Winza. Dimitri Mantheakis (Ruvu Gemstone Mining Ltd., Dar es Salaam, Tanzania) is thanked for guiding author BML's visit to Winza, and also for donating samples of Winza ruby to GIA for examination. Field support and information were also provided by Vivian Komu (Ministry of Energy and Minerals, Dodoma, Tanzania). C.H. Lapidaries Ltd. Part. (Bangkok), Paul Wild OHG (Kirschweiler, Germany), and Mushan International (Colombo, Sri Lanka) kindly donated samples to the Gübelin Gem Lab for this study. Mingling Zeng performed UV-Vis-NIR, FTIR, and EDXRF at the Gübelin Gem Lab. We thank Dr. A. Beran and Dr. E. Libowitzky (Department of Mineralogy and Crystallography, University of Vienna, Austria) for supplying useful data and discussion on FTIR spectroscopy. George Bosshart (Zürich, Switzerland) kindly reviewed the gemological and analytical parts of this study. Dr. O. Medenbach and Dr. H.-J. Bernhardt (University of Bochum, Germany) kindly performed X-ray diffraction and electron microprobe analyses of some inclusions and associated minerals. The authors are also grateful to Günther Blass (Eschweiler, Germany) for X-ray diffraction and SEM analysis of associated minerals. The slabs in figure 9 were prepared by Cedric Demeurie (UHP, Nancy). Gem dealers Werner Radl (Mawingu Gems, Niederwörresbach, Germany), Mark Kaufman (Kaufman Enterprises, San Diego), Michael Nemeth (San Diego), and Hakimi & Sons (New York) kindly loaned Winza samples for examination.

REFERENCES

Abduriyim A., Kitawaki H. (2008) New geological origin: Ruby from Winza of Tanzania. *Gemmology*, Vol. 39, Issue 8, No. 467, pp. 4–7 [in Japanese with English insert].

Appel P., Möller A., Schenk V. (1998) High-pressure granulite facies metamorphism in the Pan-African Belt of eastern Tanzania: P-T-t evidence against granulite formation by continent collision. *Journal of Metamorphic Geology*, Vol. 16, pp. 491–509.

Balmer W., Leelawatanasuk T., Atichat W., Wathanakul P., Somboon C. (2006) Update on FTIR characteristics of heated and unheated yellow sapphire. *GIT2006: 1st International Gem and Jewelry Conference*, Bangkok, December 6–7, p. 91.

Beran A., Rossman G.R. (2006) OH in naturally occurring corundum. *European Journal of Mineralogy*, Vol. 18, pp. 441–447.

Bauer M. (1896) Ueber das Vorkommen der Rubine in Birma. *Neues Jahrbuch für Mineralogie, Geologie und Paläontologie*, Vol. 11, pp. 197–238.

Berman R.G. (2007) winTWQ (version 2.3): A software package for performing internally-consistent thermobarometric calculations. *Geological Survey of Canada, Open File 5462*, 41 pp.

Choudhary G. (2008) Gem News International: An interesting zoned sapphire crystal from Winza, Tanzania. *Gems & Gemology*, Vol. 44, No. 3, pp. 270–272.

Dill H.G. (2005) Geologie und Petrographie des Saphir- und Rubinvorkommens von Chimwadzulu Hill (W-Malawi). *Gemmologie: Zeitschrift der Deutschen Gemmologischen Gesellschaft*, Vol. 54, No. 1, pp. 7–20.

Dirlam D.M., Misiorowski E.B., Tozer R., Stark K.B., Bassett A.M. (1992) Gem wealth of Tanzania. *Gems & Gemology*, Vol. 28, No. 2, pp. 80–102.

Fritz H., Tenczer V., Hauzenberger C.A., Wallbrecher E., Hoinkes G., Muhongo S., Mogessie A. (2005) Central Tanzanian Tectonic Map (CTTM): A step forward to decipher pre-Pan-African and Pan-African structural events in the East African Orogen. *Tectonics*, Vol. 20, pp. 1–45.

Gabert G., Wendt I. (1974) Datierung von granitischen Gesteinen im Dodoman- und Usagaran System und in der Ndembera-Serie (Tanzania). *Geologisches Jahrbuch*, Vol. B11, pp. 3–55.

GIT [Gem and Jewelry Institute of Thailand] Gem Testing Laboratory (2008) Rubies from a new deposit in Tanzania. www.git.or.th/eng/eng_gem_and_jewelry_database/eng_lab_notes/2008/eng_ruby_from_tanzania.htm, June 5.

Giuliani G., Fallick A.E., Garnier V., France-Lanord C., Ohnenstetter D., Schwarz D. (2005) Oxygen isotope composition as a tracer for the origins of rubies and sapphires. *Geology*, Vol. 33, pp. 249–252.

Giuliani G., Fallick A.E., Rakotondrazafy M., Ohnenstetter D., Andriamamonjy A., Rakotosamizanany S., Ralantoarison Th., Razanatseheno M., Dunaigre Ch., Schwarz D. (2007) Oxygen isotope systematics of gem corundum deposits in Madagascar: Relevance for their geological origin. *Mineralium Deposita*, Vol. 42, pp. 251–270.

Goldschmidt V. (1918) *Atlas der Krystallformen*, Vol. 5. Carl Winters Universitätsbuchhandlung, Heidelberg, Germany.

Hänni H. (1987) On corundum from Umba Valley, Tanzania. *Journal of Gemmology*, Vol. 20, No. 5, pp. 278–284.

Hänni H.A., Schmetzer K. (1991) New rubies from the Morogoro area, Tanzania. *Gems & Gemology*, Vol. 27, No. 3, pp. 156–167.

Hänni H., Krzemnicki M. (2008) New rubies from Tanzania. *Gems & Jewellery*, Vol. 17, No. 3, pp. 8–9.

Hauzenberger C.A., Bauernhofer A., Hoinkes G., Wallbrecher E., Mathu E. (2004) Pan-African high pressure granulites from SE-Kenya: Petrological and geothermobarometric evidence for polyphase evolution in the Mozambique Belt. *Journal of African Earth Sciences*, Vol. 40, pp. 245–268.

Hauzenberger C.A., Sommer H., Fritz H., Bauernhofer A., Kröner A., Hoinkes G., Wallbrecher E., Thöni M. (2007) SHRIMP U-Pb zircon and Sm-Nd garnet ages from the granulite facies basement of SE-Kenya: Evidence for Neoproterozoic polycyclic assembly of the Mozambique belt. *Journal of the Geological Society*, Vol. 164, pp. 189–201.

Henn U., Bank H., Bank F.H. (1990) Red and orange corundum (ruby and padparadscha) from Malawi. *Journal of Gemmology*, Vol. 22, No. 2, pp. 83–89.

Hughes R. (1997) *Ruby and Sapphire*. RWH Publishing, Boulder, CO.

Krzemnicki M., Hänni H.A. (2008) New Tanzania mine uncovers source of exceptional rubies. *InColor*, Spring 2008, pp. 46–47.

Melczer G. (1902) Ueber einige krystallographische Constanten des Korund. *Zeitschrift für Krystallographie und Mineralogie*, Vol. 35, pp. 561–581.

Mercier A., Debat P., Saul J.M. (1999) Exotic origin of the ruby deposits of the Mangari area in SE Kenya. *Ore Geology Reviews*, Vol. 14, pp. 83–104.

Milisenda C.C., Henn U., Bank H. (1997) The new Tunduru-Songea gem fields, southern Tanzania. *26th International Gemological Congress*, Idar-Oberstein, Germany, September 27–October 3, pp. 37–39.

Moeller A., Mezger K., Schenk V. (2000) U-Pb dating of metamorphic minerals: Pan-African metamorphism and prolonged slow cooling of high pressure granulites in Tanzania, East Africa. *Precambrian Research*, Vol. 104, pp. 123–146.

Pardieu V. (2005) An update on ruby and sapphire mining in South East Asia and East Africa—Summer 2005. www.fieldgemology.org.

Pardieu V. (2007) Tanzania, October 2007—A gemological safari. Part 1: Ruby, sapphire, moonstone, spinels, tsavorite, alexandrite: Gems from Central and South Tanzania. www.fieldgemology.org.

Pardieu V., Schwarz D. (2008) Field report from Winza. *Rapaport Diamond Report*, Vol. 31, No. 26, pp. 173–175.

Peretti A., Schmetzer K., Bernhardt H.-J., Mouawad F. (1995) Rubies from Mong Hsu. *Gems & Gemology*, Vol. 31, No. 1, pp. 2–26.

Peretti A. (2008) New important ruby discovery in Tanzania: The Tanzanian "Winza"-(Dodoma province) rubies. *Contributions to Gemmology*, No. 7, April, www.gemresearch.ch/news/Tanzania/Tanzania.htm.

Peucat J.J., Ruffault P., Fritsch E., Bouhnik-Le Coz M., Simonet C., Lasnier B. (2007) Ga/Mg ratio as a new geochemical tool to differentiate magmatic from metamorphic blue sapphires. *Lithos*, Vol. 98, pp. 261–274.

Rankin A.H., Greenwood J., Hargreaves D. (2003) Chemical fingerprinting of some East African gem rubies by laser ablation ICP-MS. *Journal of Gemmology*, Vol. 28, No. 8, pp. 473–482.

Schwarz D., Stern W., Zachovay M. (2000) Trace and minor element contents in synthetic rubies from different manufacturers. *31st International Geological Congress*, Rio de Janeiro, Brazil, August 6–17.

Schwarz D. (2001) Sapphires and rubies from the Ruvuma (Tunduru and Songea), Lindi (Liwale) and Mtwara (Mbekenyera) districts in southern Tanzania. *28th International Gemmological Congress*, Madrid, Spain, October.

Senoble J.B. (2008) An expedition to Tanzania's new ruby deposits in Winza. *InColor*, Spring 2008, pp. 42–43.

Sharp Z.D. (1990) A laser-based microanalytical method for the in-situ determination of oxygen isotope ratios of silicates and oxides. *Geochimica et Cosmochimica Acta*, Vol. 54, pp. 1353–1357.

Simonet C. (2000) Géologie des gisements de saphir et de rubis. L'exemple de la John Saul mine, Mangari, Kenya. Ph.D. dissertation, University of Nantes, France.

Smith C.P., Van der Bogert C. (2006) Infrared spectra of gem corundum. *Gems & Gemology*, Vol. 42, No. 3, pp. 92–93.

Smith C.P., Beesley C.R., Quinn Darenius E., Mayerson W.M. (2008) Inside rubies. *Rapaport Diamond Report*, Vol. 31, No. 47, pp. 140–148.

Sommer H., Kröner A., Hauzenberger C.A., Muhongo S. (2005) Reworking of Archaean and Palaeoproterozoic crust in the Mozambique Belt of central Tanzania as documented by SHRIMP zircon geochronology. *Journal of African Earth Science*, Vol. 43, pp. 447–463.

SSEF Swiss Gemmological Institute (2008) New rubies from Tanzania. *SSEF Newsletter*, May, www.ssef.ch/en/news/news_pdf/SSEFnewsletter_may08.pdf.